From the department of Nephrology, Heinrich Heine University Düsseldorf

Potassium intake induces cardiovascular damage in hypertensive *Apoe*$^{-/-}$ mice under high sodium conditions

Dissertation

to obtain the academic title of Doctor of Philosophy (PhD) in Medical Sciences from the Faculty of Medicine at Heinrich Heine University Düsseldorf

submitted by

Denada Arifaj

2024

As an inaugural dissertation printed by permission of the
Faculty of Medicine at Heinrich Heine University Düsseldorf

Dean: Prof. Dr. med. Nikolaj Klöcker

Examiners: Prof. Dr. med Johannes Stegbauer
Prof. Dr. Norbert Gerdes

“If it does not challenge you, it won’t change you.”

-Fred Devito

Summary

Increased sodium intake aggravates cardiovascular diseases by modulating blood pressure and immune cell response. Studies reveal that sodium substitute containing potassium protects from cardiovascular morbidity and mortality in hypertensive patients with high cardiovascular risk. In this work, we investigate the role of high potassium (K^+ 5%) intake on the development of hypertensive cardiac damage in the presence or absence of high sodium diet. Throughout the whole trial, apolipoproteinE-deficient mice (*Apoe*$^{-/-}$) were fed a normal K^+ (0,55%) or high K^+ (5%) diet. *Apoe*$^{-/-}$ mice were infused with angiotensin (Ang) II (500ng/kg/min) for 28 days starting two weeks after the start of the diet. In a second series of experiments, 1% sodium (Na^+) was added to the drinking water of high K^+-fed mice. Magnetic Resonance Imaging (MRI), immunohistochemistry, flow cytometry analysis, quantative PCR and Western blot were used to assess the cardiac damage. High K^+ diet increased serum potassium levels significantly, compared to mice treated with normal K^+ diet, but had no impact on blood pressure or cardiac function in *Apoe*$^{-/-}$ mice chronically infused with Ang II. Anticipated, aldosterone excretion was significantly increased in Ang II infused *Apoe*$^{-/-}$ mice fed a high K^+ diet compared to a normal K^+ diet. To evaluate the consequence of potassium mediated aldosterone secretion for hypertensive cardiovascular damage, we additionally treated our high K^+ groups with high Na^+. Potassium-induced aldosterone production in the setting of high sodium exaggerates hypertensive cardiac damage. High K^+/high Na^+-fed mice had significantly higher left ventricular mass, more cardiac fibrosis and lower ejection fraction in comparison to high K^+ or high Na^+ fed mice. Furthermore, inflammation and a consequent premature senescence associated secretory phenotype were linked to cardiac injury. Therefore, the simultaneous intake of high K^+ and high Na^+ diet, induced higher mitochondrial ROS production in different cardiac cell types compared to high K^+ or high Na^+ diet. The *Apoe*$^{-/-}$ mice fed with high K^+/high Na^+ had greater levels of cellular senescence biomarkers such as p16 and p21. Notably, co-treatment with spironolactone (50mg/kg/day), a mineralocorticoid receptor antagonist (MRA), significantly attenuated cardiovascular damage in mice fed a high K^+/high Na^+ diet. In conclusion, the data from this study demonstrate that not only does a high K^+ intake have no beneficial effect on blood pressure and cardiovascular health in hypertensive mice, but it might also have negative effects if it is combined with a high Na^+ diet.

Zusammenfassung

Eine erhöhte Natriumzufuhr verschlimmert Herz-Kreislauf-Erkrankungen durch erhöhten Blutdruck. In dieser Studie untersuchten wir die Rolle einer hohen Kaliumzufuhr (K^+ 5 %) bei der Entwicklung von hypertensiven Herzschäden in Gegenwart oder Abwesenheit einer natriumreichen Ernährung. Apolipoprotein E-defiziente Mäuse ($Apoe^{-/-}$) wurden während des gesamten Versuchszeitraums mit einer normalen K^+ (0,55 %) oder einer Diät mit hohem K^+ (5 %) gefüttert. Zwei Wochen nach Beginn der Diät wurden die $Apoe^{-/-}$-Mäuse 28 Tage lang mit Angiotensin (Ang) II (500ng/kg/min) infundiert. Die hypertensiven Herzschäden wurden mittels MRT, Durchflusszytometrie und quantitativer PCR untersucht. Hohe K^+-Diät erhöhte den Serumkaliumspiegel im Vergleich zu Mäusen, die mit einer normalen K^+-Diät behandelt wurden, hatte jedoch keine Auswirkungen auf den Blutdruck oder die Herzfunktion von $Apoe^{-/-}$-Mäusen. Wie erwartet war die Aldosteronausscheidung bei $Apoe^{-/-}$ Mäusen, die mit Ang II infundiert wurden und ein K^+- erhielten, im Vergleich zu Mäusen mit einer normalen K^+- Diät signifikant erhöht. Um die Folgen der Aldosteronausscheidung für hypertensive kardiovaskuläre Schäden zu untersuchen, behandelten wir die Gruppe mit hoher K^+-Diät mit einer Diät mit hohem Natriumgehalt (1 % Na^+), um zu zeigen, dass die K^+ -vermittelte Aldosteronproduktion hypertensive kardiale Schäden bei hohem Na^+ verschlimmert. Herz-MRT und Immunhistochemie zeigten eine signifikante linksventrikuläre Herzfibrose und eine geringere Auswurffraktion sowie eine höhere Expression von Entzündungsmarkern im Vergleich zu hohem K^+ oder hohem Na^+. Darüber hinaus wurden die kardiovaskulären Schäden mit oxidativem Stress und einer daraus resultierenden vorzeitigen zellulären Seneszenz im Herzen in Verbindung gebracht. So führte die gleichzeitige Aufnahme einer Diät mit hohem K^+/Na^+-Gehalt zu einer höheren mitochondrialen ROS-Produktion in verschiedenen Herzzelltypen im Vergleich zu einer Diät mit hohem K^+- oder hohem Na^+-Gehalt. Biomarker der zellulären Seneszenz wie p16 und p21 waren bei $Apoe^{-/-}$-Mäusen, die eine hohe K^+/Na^+-Diät erhielten, signifikant erhöht. Bemerkenswert ist, dass die gleichzeitige Behandlung mit Spironolacton (50 mg/kg/Tag), einem Mineralokortikoidrezeptor-Antagonisten, die kardiovaskulären Schäden und die zelluläre Seneszenz bei Mäusen, die mit einer K^+/Na^+-Diät gefüttert wurden, signifikant verringerte. Zusammenfassend zeigt diese Studie nicht nur, dass eine hohe K^+-Zufuhr keine positiven Auswirkungen auf den Blutdruck und die kardiovaskuläre Gesundheit bei hypertensiven Mäusen hat, sondern auch, dass sie schädliche Auswirkungen haben kann, wenn sie mit einer hohen Natriumzufuhr einhergeht.

Abbreviations

Ang II: Angiotensin II

ANP: Atrial Natriuretic Peptide

AP-1: Activator Protein 1

Apoe $^{-/-}$: Apolipoprotein E gene deficiency

ASDN: Aldosterone-Sensitive Distal Nephron

ATP: Adenosine Triphosphate

ATP5FA1: ATP synthase F1 subunit alpha

βMHC: Beta- Myosin Heavy Chain

BNP: Brain Natriuretic Peptide

BP: Blood Pressure

CD: Cluster of Differentiation

(c)DNA: (complementary) Deoxyribonucleic Acid

CKD: Chronic Kidney Diseases

CNT: Connecting Tubule

cTnT: cardiac Troponin T

COX IV: Cytochrome C Oxidase

CVD: Cardiovascular Diseases

DCT: Distal Convoluted Tubule

DNA: Deoxyribonucleic acid

DOCA: Deoxycorticosterone acetate

DWT: Diastolic Wall Thickness

ECG: Electrocardiogram

EDV: End-diastolic Volume

EF: Ejection Fraction

ESV: End-systolic Volume

ENaC: Epithelial Sodium Channels

FBS: Fetal Bovine Serum

FFPE: Formalin-Fixed Paraffin-Embedded

GAPDH: Glyceraldehyde 3-phosphate dehydrogenase

(g)DNA: (genomic) Deoxyribonucleic Acid

HSA: Human Serum Albumin

IHC: Immunohistochemistry

iNOS: inducible Nitric Oxide Synthase

IL: Interleukin

IL-1β : Interleukin 1 Beta

K^+: Potassium

LC3B: Light Chain 3B

LVM: Left Ventricular Mass

MCP1: Monocyte Chemoattractant Protein-1

MR: Mineralocorticoid Receptor

MRI: Magnetic Resonance Imaging

MS: MitoSox

MT: MitoTracker

Na^+: Sodium

NADP(H): Nicotinamide Adenine Dinucleotide Phosphate

NCC: Sodium-Chloride Cotransporter

NFκB: Nuclear Factor Kappa B

NO: Nitric Oxide

NOX2: NADPH Oxidase 2

PAI-1: Plasminogen Activator Inhibitor 1

PBS: Phosphate-Buffered Saline

PCR: Polymerase Chain Reaction

PEEK: Polyether Ether Ketone

PFA: Paraformaldehyde

RAAS: Renin Angiotensin Aldosterone System

RNA: Ribonucleic Acid

RT: Room Temperature

ROS: Reactive Oxygen Species

SASP: Senescence Associated Secretory Phenotype

SBP- Systolic Blood Pressure

SDS-PAGE: Sodium Dodecyl Sulphate – Polyacrylamide Gel Electrophoresis

SOD2: Superoxide Dismutase 2

SWT: Systolic Wall Thickness

OPA1: Optic Atrophy 1

TGFβ: Transforming Growth Factor Beta

TNFα: Tumor Necrosis Factor Alpha

TVM: Total Ventricular Mass

WNK: With-no-lysine (K)

WGA: Wheat Germ Agglutinin

Table of Content

1. Introduction

1.1. CVD and diet pattern

Chronically elevated blood pressure (BP) is a major factor for cardiovascular diseases (CVD) and the leading cause of preventable mortality worldwide, accounting for 11.3 million deaths overall in 2021 (Vaduganathan et al. 2022. J Am Coll Cardiol). Hypertension-induced cardiovascular deaths have been linked to ischemic heart diseases and stroke (Vaduganathan et al. 2022. J Am Coll Cardiol) (Figure 1). Many clinical guidelines which aim to implement various BP-lowering strategies through pharmacological and non-pharmacological interventions. Diet has a strong influence on BP. Excess dietary sodium (Na^+) has been associated with hypertension, and restriction of sodium intake by 2,3 grams/day can decrease the cardiovascular events and the death rate (Greer et al. 2019. Hypertension). Epidemiological (Mente et al. 2014. N Engl J Med) and interventional studies have shown that dietary potassium (K^+) intake not only lowers BP but modulate the salt sensitivity. Potassium adequate intake level of 3,4 grams/day can reduce BP in hypertensive patients particularly.

Figure 1

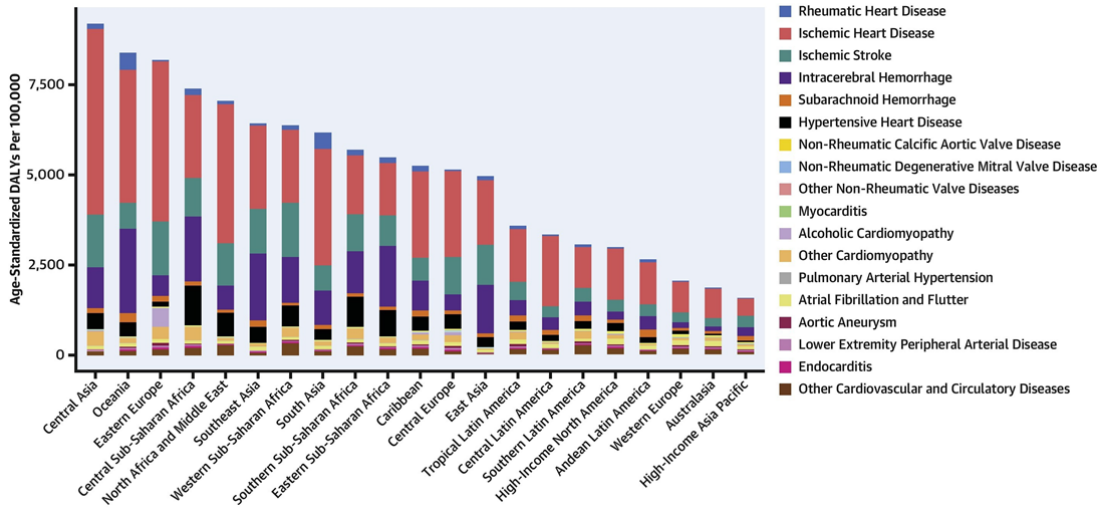

Fig.1: Global ranking of cardiovascular deaths by cause. Specific cardiovascular diseases by region in 2022. Source: Global Burden of Cardiovascular Diseases and Risks Collaboration, 1990-2021.

1.2. Effect of potassium intake on blood pressure

There has been growing interest in public health strategies in reducing Na^+ and increasing K^+ to improve cardiovascular health. Several optimal intervention strategies have been advocated such as potassium supplementation, use of sodium substitution with K^+, and/or simply to increase the K^+ rich diet (i.e. fruits, legumes).

Experimental studies in humans suggest that potassium supplementation may decrease blood pressure particularly in adults with hypertension (Riphagen et al. 2016. J Hypertens; Nomura et al. 2019. Clin Exp Nephrol). A meta-analysis from Iqbal et al. (2019. Nutrients) showed that the increase in K^+ intake exerted a reduction of systolic blood pressure (SBP) of 8 to 9 mmHg in adults with higher baseline sodium excretion and a lower potassium excretion. The same finding was demonstrated by (Filipini et al. 2017. Int J Cardiol) that a BP lowering effect is achieved by a 90 mmol/day potassium intake. Conversely, normotensive adults subjected to dietary K^+ depletion reported a SBP increase of 10mmHg (Krishna et al. 1991. Ann Intern Med). Notably, a recent meta-analysis of 32 randomized-controlled trials (duration 4 weeks) explored the dose-response relationship between potassium supplementation and BP (Filippini et al. 2020. J Am Heart Assoc). They observed a U-shaped relationship, showing that a K^+ intake lower than 30 mmol/day or over 80 mmol/day increases SBP. Particularly excessive amounts of potassium should be avoided from the subjects that take antihypertensive medication which are associated with high plasma potassium levels. Additionally, plasma potassium stimulates the secretion of BP-raising hormone aldosterone (Figure 2). A drop in renal perfusion volume or reduced sodium delivery to the kidney triggers the renin release from juxtaglomerular cells (Reincke et al. 2021. Lancet Diabetes Endocrinol). Renin converts the liver-derived angiotensinogen to angiotensin I (Ang I), which is further converted to angiotensin II (Ang II) by angiotensin-I-converting enzyme on the surface of endothelial cells. Ang II triggers the secretion of aldosterone hormone by zona glomerulosa cells of adrenal gland (Figure 2). Further the secreted aldosterone binds to mineralocorticoid receptor (MR) in aldosterone-sensitive distal nephron (ASDN) to induce sodium re-absorption and increase plasma volume and consecutively elevates blood pressure. Therefore, there is a limitation to consider potassium supplementation as a population-wide approach, because it cannot be applicable in all settings due to baseline sodium and potassium intake.

Dietary guidelines mutually advise reduced Na^+ intake and increased K^+ intake concomitantly to control BP. Therefore, sodium substitute with potassium has emerged as a

promising alternative for controlling blood pressure and lowering cardiovascular risk. Sodium substitute is available as a single product in which potassium is replaced for ≤30% of pure sodium (Jones et al. 2022. Hypertension). Remarkably, Salt Substitute Stroke Study (SSaSS) has provided some significant insights (Neal et al. 2021. N Eng J Med). The trial involved 20,995 persons in 600 villages of China, above 65,4 years old and had a previous history of hypertension, stroke and cardiovascular diseases. The villages were randomly assigned participants who received the sodium substitute (75% Na and 25% K), and participants who continued to use regular sodium (100% Na) in a course of 5 years. Sodium substitute significantly lowered the rate of stroke, cardiovascular events by 13% and death by 12%. The rate of adverse clinical outcomes concerning hyperkalemia was the same as in regular sodium consumers. Regarding the hyperkalemic episodes as a result of increased potassium intake, the India modelling study addressed this issue by evaluating the risk and benefits of sodium substitute in patients with chronic kidney diseases (CKD). They found out that cardiovascular benefits outweigh the hyperkalemia risk (Marklund et al. 2022. J Hypertens). A new study was conducted in 48 residential elderly care facilities of China, where participants were 2 x 2 cluster randomised to sodium substitute (62.5% Na and 25% K) versus usual sodium and to progressively restricted versus to usual supply of sodium for 2 years (Yuan et al. 2023. Nat Med). They showed that sodium substitute compared with regular sodium reduced SBP by 7 mmHg and diastolic blood pressure by 1.9 mmHg, whereas the restricted sodium supply did not affect BP. Sodium substitute also reduced cardiovascular events, although no effect was observed in total mortality. Mean serum potassium levels increased with sodium substitute use, but was not associated with adverse clinical outcomes. This study reinforces the beneficial effect of sodium substitutes to decrease blood pressure and provides reassurance on safety in high-risk populations (McLean. 2023. Nat Med).

Figure 2

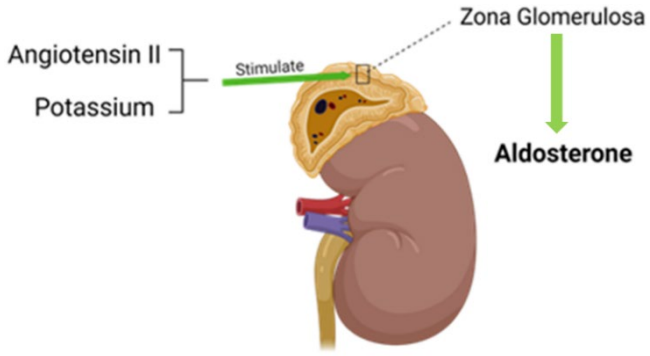

Fig.2: Aldosterone secretion from adrenal gland. Angiotensin II stimulates zona glomerulus of adrenal gland, leading to aldosterone secretion.

1.3. Potassium switch

On average, K^+ is 50–55 mmol/kg body weight, much less compared to palaeolithic times when dietary potassium was much higher (250-400 mmol/day) (Sebastian et al. 2006. Semin Nephrol; Kamel et al. 2014. Nephrol Dial Transplant). The Na^+-K^+-ATPase of every cell ensures a maintenance of high intracellular potassium concentration (120-140 mM) and low extracellular potassium concentration (3.5-5.0 mM). This strict range is vital for not disturbing the resting membrane potential of cells, because hyper- or hypokalemia causes muscle paralysis and cardiac arrhythmia (McDonough et al. 2022. Eur J Physiol). After a K^+-rich meal, potassium is reallocated to the intracellular compartment from extracellular fluid and excreted proportionally by the kidneys. This way, the plasma potassium level is maintained at 3.5 to 5.0 mmolL through internal and external mechanisms. The kidney plays a crucial role by matching potassium excretion with dietary intake. Around 90% of unbound potassium is reabsorbed by the kidney, while the rest reaches the distal nephron (Zacchia et al. 2016. Kidney Dis).

The distal nephron is recognized for sodium reabsorption and potassium secretion, making it a critical site for potassium excretion. It consists of distal convoluted tubule (early DCT and late DCT), the connecting tubule (CNT) and collecting duct. The late DCT and CNT is referred to as aldosterone-sensitive distal nephron (ASDN). The electroneutral chloride cotransporter (NCC) facilitates sodium reabsorption in early DCT and epithelial sodium channels (ENaC) modulate sodium reabsorption in ASDN. The electrogenic reabsorption of sodium by ENaC coupled with ROMK form the main secretory route of potassium secretion (Valinsky et al. 2018. Clin Sci). High K^+ diet increases the potassium secretion, while a depletion of K^+ diet shifts from secretion to reabsorption of potassium (Gumz et al. 2015. N Engl J Med). Alterations in sodium reabsorption affect potassium secretion, which is highlighted in primary aldosteronism and Gitelman syndrome patients. Overactivation of NCC leads to K^+ retention and hyperkalemia, while loss of NCC function results in K^+ wasting and hypokalemia (Wilson et al. 2001. Science).

Recent studies have identified a kidney potassium switch within the distal nephron (Terker et al. 2015. Cell Metab; Wang et al. 2018. Kidney International; Cuevas et al. 2017. JASN). This switch turns NCC off and ENaC on in response to high K^+ intake (Su et al. 2020. Current Cardiology Reports). High plasma potassium concentration dephosphorylates NCC through WNK kinases cascade, thereby increasing the sodium delivery to ASDN. This leads

to activation of ENaC which increases the lumen negativity for potassium secretion. ENaC activity is further enhanced by potassium-induced aldosterone (Figure 3).

Accordingly, a high K^+ diet causes sodium excretion and lower blood pressure. The counteracting effect is applicable for low K^+ intake, which increases sodium reabsorption and blood pressure.

Figure 3

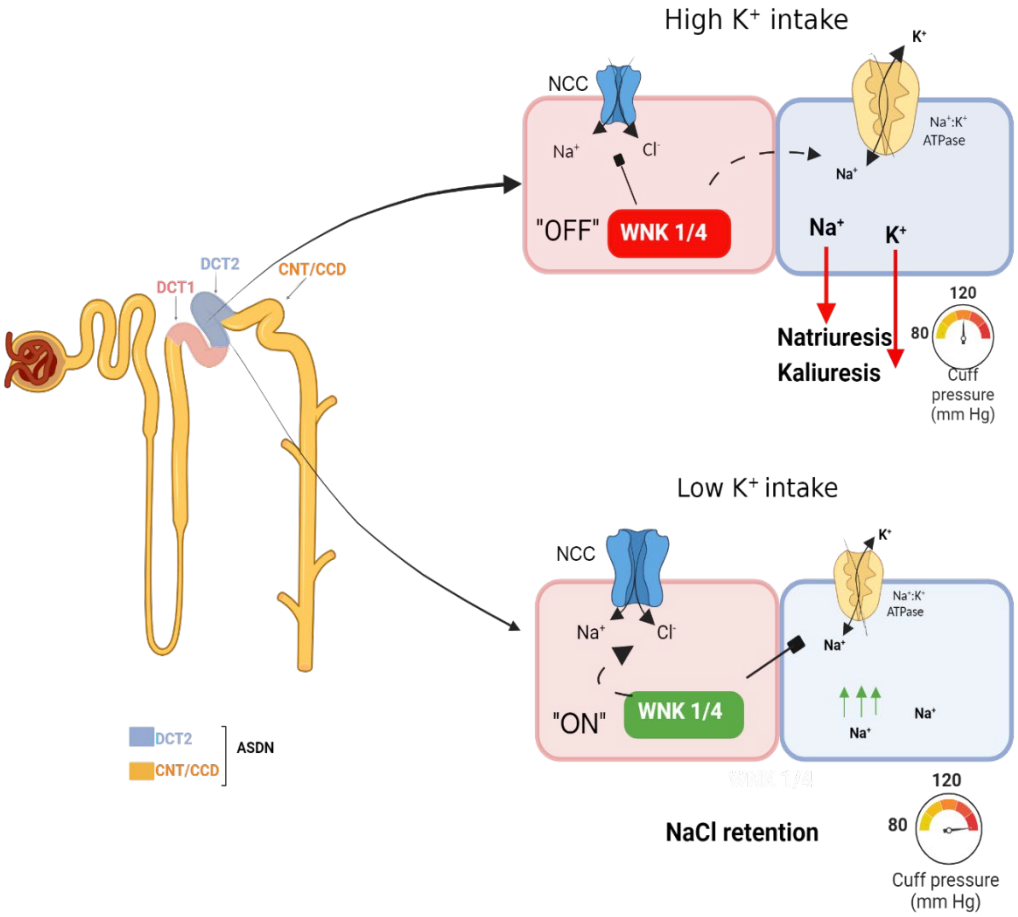

Fig.3: Low plasma potassium activates the WNK4 kinase by hyperpolarizing the membrane, which in turn phosphoactivates NCC in DCT1. Thereby it causes sodium retention and limits sodium delivery to ASDN (DCT2+CNT), which further reduces potassium excretion. The system is activated by low potassium even in high sodium presence, on this way leading to salt sensitivity and hypertension. Meanwhile, high plasma potassium turns off the switch in DCT1. This leads to increased sodium delivery to ASDN and excretion, resulting in lower blood pressure. The illustration was drawn by using Biorender application and adapted from Su et al. 2020. Current Cardiol Reports.

1.4. Aldosterone paradox

High dietary K^+ intake lowers the blood pressure but also increases aldosterone secretion by zona glomerulosa cells of the adrenal gland. In addition to its classic role in increasing blood pressure through increased sodium retention and potassium excretion in the kidneys, aldosterone modulates pathophysiological processes in the cardiovascular system by binding to the mineralocorticoid receptor (MR) (Buffolo et al. 2022. Hypertension). MRs are expressed in non-epithelial cells such as cardiomyocytes, endothelial cells, vascular smooth muscle cells, fibroblasts and inflammatory cells (Brown et al. 2013. Nat. Rev. Nephrol). Abnormal MR activation contributes to cardiovascular alterations such as cardiac inflammation, fibrosis and myocardial hypertrophy.

Aldosterone and/or MR activation generate reactive oxygen species (ROS) which activate the proinflammatory transcription factors activator protein (AP)-1 and nuclear factor kappa B (NFκB). It is shown that aldosterone increases nicotinamide adenine dinucleotide phosphate [NADP(H)] oxidase (NOX) activity and oxidative stress in the heart (Brown et al. 2013. Nat. Rev. Nephrol). Macrophages also play an important role in inflammation. Compelling studies have reported that macrophage-specific deletion of *Nr3C2*, the gene encoding MR, protects mice against interstitial and perivascular cardiac fibrosis induced by DOCA plus salt (Rickard et al. 2009. Hypertension). The chronic inflammation is followed by proliferation of myofibroblasts, collagen production, perivascular and interstitial fibrosis (Jones et al. 2021. Hypertension). Aldosterone increases TGF-β1 in cultured cardiomyocytes and in the hearts of mice aldosterone-MR binding contribute directly to cardiomyocyte hypertrophy (Figure 4) (Parksook et al. 2023. Cardiovascular Research).

Along with fibrosis, chronic inflammation is a potential risk for senescence associated secretory phenotype (SASP) and ROS mediated cellular senescence. Cellular senescence is characterised by a permanent cell-cycle arrest, typically occurring in the G1 or G2 phase, which serves as a safeguard mechanism to prevent the proliferation of damages or potentially harmful cells. The main trigger of cellular senescence is DNA damage which activates the DNA damage response and p53-p21 pathway. Further, epigenetic alterations activate p16-RB pathway, which helps to maintain the senescence state. SASP is a hallmark feature of senescent cells which involves the secretion of variety pro-inflammatory cytokines like IL-6. Additionally, elevated oxidative stress caused by overproduction of ROS can induce cellular senescence by reducing the DNA copying and modulating SASP. ROS causes oxidative damage to mitochondrial and cellular DNA due to mitochondria malfunction

(Mylonas et al. 2022. Front. Aging). Aldosterone induced mitochondrial ROS has been more studied in mesangial cells, where rotenone reverses the aldosterone renal injury and lowers the blood pressure (Yuan et al. 2012. Free Radic Biol Med). Mitochondrial dysfunction has been associated with cardiac remodelling, but the role of aldosterone on mitochondria remains unclear. A recent study demonstrated that aldosterone downregulated mitochondrial DNA, superoxide dismutase 2 mitochondrial (SOD2) and cytochrome c oxidase (COX IV) protein through an MR/MAPK/p38 pathway and ROS production (Tsai et al. 2021. Biomedicines). Considering the MR expression in T cells and macrophages, chronic inflammation can lead also SASP. This pathway involves nuclear factor kappa beta (NF-κB), interleukin 7 (IL-7) and chemokines that different cell types exchange and affect each other, in this way contributing to senescence (Labora et al. 2020. Trends Cel Biol).

Mounting evidence has supported the link of aldosterone dependent and independent MR signalling with sodium in hypertension. Thus, typically high sodium suppresses Ang II and aldosterone production in order to keep normal BP values (Maeoka et al. 2022. Hypertension). However, observational and experimental studies have shown that the combination of sodium and aldosterone excess enhance cardiovascular morbidity (Brown. 2013. J Nat Rev Nephrol). In rats, continuous infusion of aldosterone with 1% Na^+ via drinking water resulted in arterial hypertension, proteinuria and glomerular damage (Nishiyama et al. 2004. Hypertension). Comparable results were reported in a rat model rendered hypertensive by aldosterone infusion and high sodium diet, which developed left ventricular hypertrophy and perivascular fibrosis. The aldosterone-sodium proinflammatory and profibrotic effect in kidney, vasculature and heart were prevented by MR antagonism (Blasi et al. 2003. Kidney Int; Lacolley et al. 2002. Circulation; Brilla et al. 1993J Mol Cell Cardiol). Several mechanisms could potentially explain aldosterone-sodium interaction to promote mineralocorticoid-induced organ damage. Schneider et al. suggest that local renin-angiotensin-aldosterone system (RAAS) and inflammation culminate on the generation of ROS, which in turn oxidize and activate the MR, leading to a transcription of MR-dependent genes and downstream organ damage (Chen et al. 2023. Hormone and Metabol Research). It is also reported the MR antagonism decreases inflammation and fibrosis during high sodium intake, despite low aldosterone levels, suggesting activation of MR independently of aldosterone. It is evident that increased Rac1, Rho family GTPase, may activate MR during high sodium intake to elevate the BP (Maaliki et al. 2022. Front Physiol). However,

the mechanism remains unclear. These countervailing effects have led to debates and disagreements about the optimal dietary intake.

Figure 4

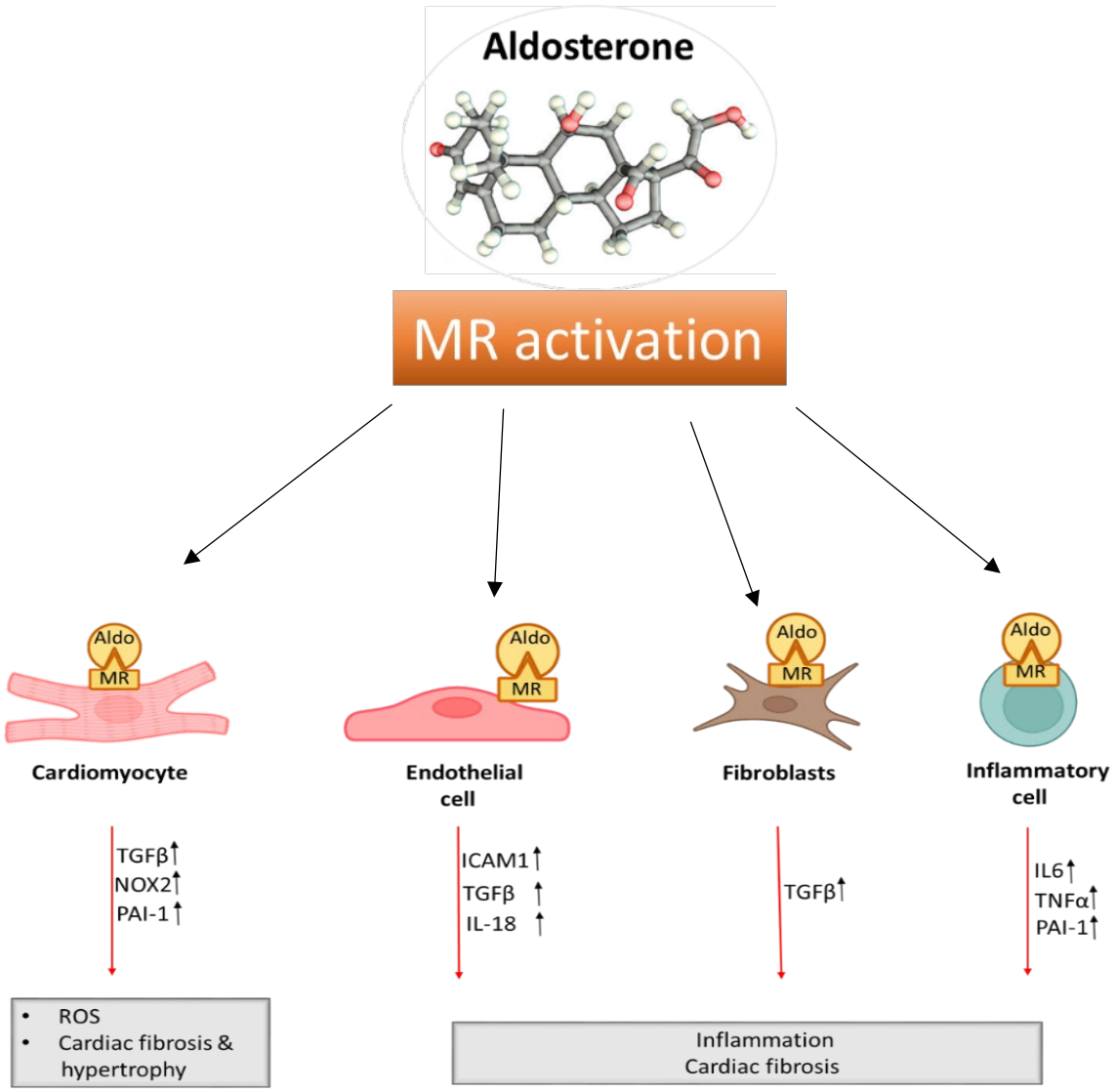

Fig.4: Effects of cell-specific activation of the MR in the heart. Aldosterone activates the MR on cardiomyocytes to produce ROS, fibrosis and hypertrophy in the heart. In the endothelial cells, MR activation by aldosterone increases the production of ICAM1, TGFβ and IL-18. Aldosterone activates MR in fibroblast and inflammatory cells to promote inflammation and cardiac fibrosis. The illustration was drawn by using Biorender application and adapted from Parksook et al. 2023. Cardiovasc. Res.

1.5. Sodium and Hypertension

High Na^+ has been associated with elevated blood pressure and consequently an increase in cardiovascular risk and death (Wainford. 2017. Hypertension). Several reports have presented a positive, independent linear relationship between BP and 24h urinary sodium excretion (Ellison et al. 2021. N Engl J Med). The World Health Organization recommends a daily sodium consumption less than 2g/day. However, not all individuals respond equally to Na^+ intake, which is known as salt-sensitivity. In this regard, some patients exhibit high blood pressure values when challenged with Na^+ load, while Na^+ depletion causes a significant decrease of BP (Elijovic et al. 2016. Hypertens).

The pathophysiological link between sodium intake and increase in BP has been widely debated. Different hypothesis has been extensively investigated such as:

Altered renal mechanism/volume-loading theory by Guyton, shows that Na^+ administration increases the water retention, hence the intravascular volume which leads to an increase in cardiac output and kidney perfusion pressure (Guyton et al.1972 Annu Rev Physiol). The rise in kidney perfusion pressure increases the sodium excretion to achieve the fluid balance in the body. If the kidney loses the ability to excrete excessive sodium and fluid volume, the pulse volume and BP increase consequently (Balafa et al. 2020. J Hum Hypertens).

Enhanced activation of the sympathetic nervous system and disturbances in nitric oxide (NO) activity mediate impaired vasodilatory response to sodium that increases blood pressure (MorrisJr et al. 2016. Circulation).

Another mechanism is immune system-mediated response related to skin hypertonicity. High sodium diet results in Na^+ and Cl^- storage in the skin causing a local hypertonic environment. The osmotic stress triggers homeostatic macrophages to exert blood pressure-regulatory effect via tonicity-responsive enhancer-binding protein (TONEBP)-driven modulation of cutaneous lymphatic capillary function (Wiig et al. 2013. J Clin Invest; Kitada et al. 2023. Hypertension).

Recent studies have revealed that other systems such as the gut contribute to hypertension in the context of high sodium. It has been shown that high Na^+ intake affects gut microbiome by depleting Lactobacillus spp, which increased T_H17 cells and blood pressure, thereby connecting gut-immune axis with salt-sensitivity hypertension (Wilck et al. 2017. Nature).

1.6. Aim of the study

The aim of this thesis is to examine the potential benefits of increased potassium intake on blood pressure regulation in hypertension, while considering the concurrent rise in aldosterone levels. Additionally, we aim to investigate the cardiac outcomes associated with elevated potassium intake in the presence of excess sodium, using a hypertensive model featuring *Apoe*$^{-/-}$ mice infused with angiotensin II.

2. Methods

2.1. Mice and dietary manipulation

The University Hospital of Düsseldorf Animal Care and Use Committee approved the experiments for this study (G301/18; 81-02.04.2018.A301). *Apoe*$^{-/-}$ mice on a C57BL/6 background were housed in a temperature-controlled facility with a 12:12-h light-dark cycle within the central animal care of University Hospital of Düsseldorf. Food and water were available *ad libitum*. Male *Apoe*$^{-/-}$ mice (8-10 weeks old) were used in the *in vivo* experiments. In all animal models, mice were first acclimated to standard chow containing 0.55 % K^+. The following dietary protocols were performed to assess the role of dietary K^+ on cardiovascular outcomes:

1) For assessment of the beneficial effect of high K^+ diet on cardiac function, mice were randomized to two dietary groups. They received either a high K^+ diet (5%) or a control diet referred to as normal K^+ (0.55%) for 6 weeks in group cages. Diets were matched for caloric content and only differed in potassium content. Table 1 shows the electrolyte composition of these diets. Two weeks after the start of the diet, *Apoe*$^{-/-}$ mice were infused with Ang II (500ng/kg/min) minipumps for 28 days (Figure 5). During the 4 weeks of Ang II, blood pressure and MRI measurements were performed.

Figure 5

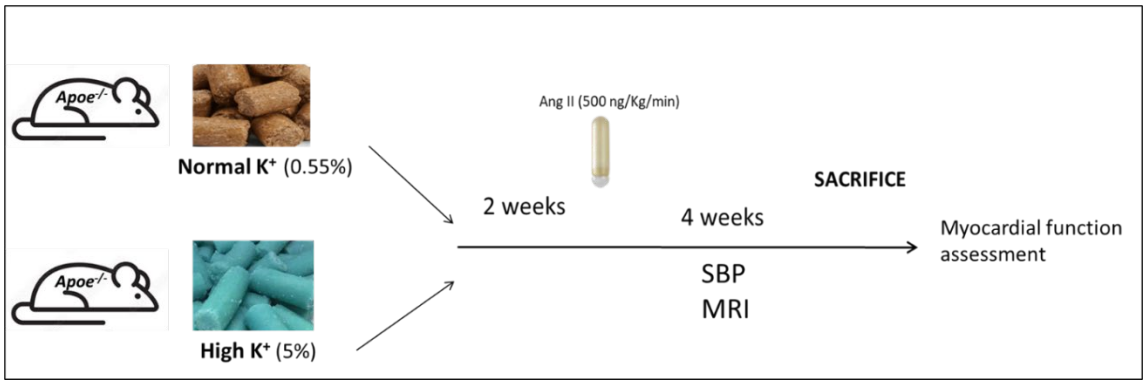

Fig.5: *Apoe*$^{-/-}$ mice were supplied with high or normal K^+ diet. SBP was measured twice per week and MRI was performed one day before the sacrifice.

2) To evaluate the significance of potassium-induced aldosterone, mice were supplemented with 1% Na^+ in the drinking water, knowing that sodium aggravates aldosterone effects. *Apoe*$^{-/-}$ mice were randomly assigned to stay on the high K^+ diet or receive high K^+ diet and high Na^+ in the drinking water concomitantly. To test the effect of high sodium, we supplied normal K^+-fed mice with high Na^+ in drinking water. The same animal model was adapted, as shown in Figure 6.

Figure 6

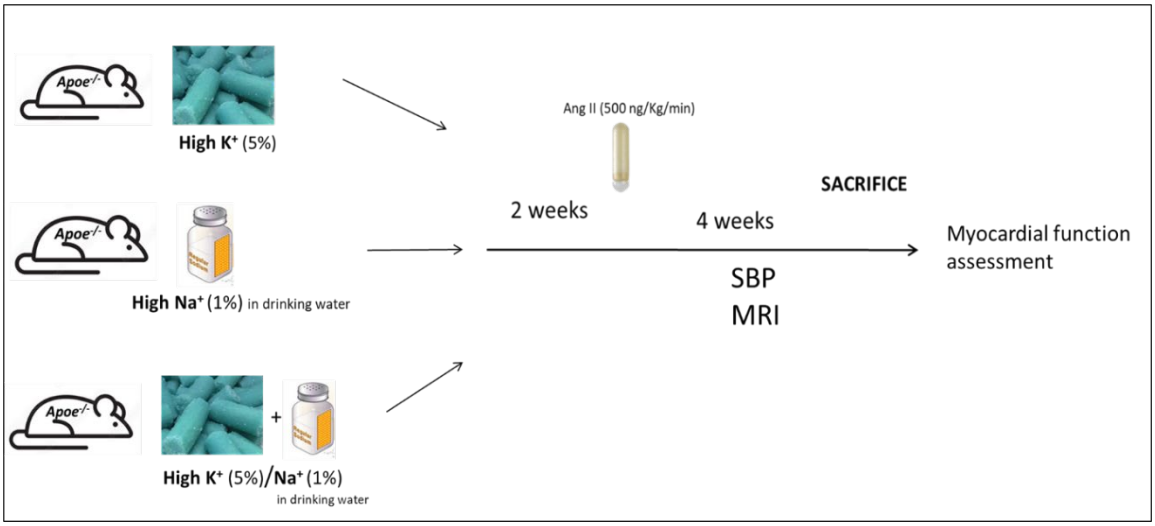

Fig.6: *Apoe*$^{-/-}$ mice were randomized to three dietary groups and received either high K^+ or high Na^+ as either high K^+/high Na^+ diet. Systolic BP and cardiac MRI measurements were performed after Ang II infusion.

3) To prove that potassium-induced aldosterone in Na^+ presence has detrimental effects on cardiac function, we blocked the mineralocorticoid receptor using spironolactone. After mice were acclimated to a standard diet, they were fed with high K^+ diet/high Na^+, receiving either spironolactone or not. The MR was blocked via the implantation of spironolactone pellets on the first day of the experiment. The same animal model was customized (Figure 7).

Figure 7

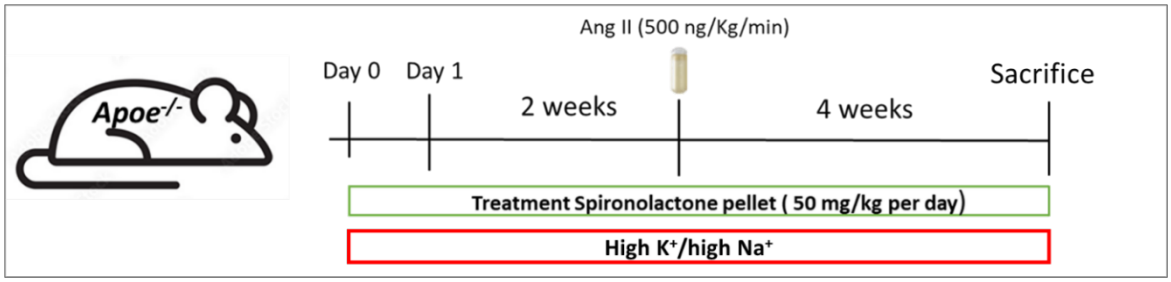

Fig.7: One day before the start of diet, *Apoe*$^{-/-}$ mice were assigned to spironolactone or placebo administered. The next day, both groups received high K^+/high Na^+ for 42 days. Ang II was infused two weeks after the initiation of the diet.

Table 1. Composition of the purified potassium diets presented as physiological fuel

Ingredients		0.55% K^+ Normal K^+	5% K^+ High K^+
Proximate content			
Potassium	%	0.55	5.0
Sodium	%	0.16	0.16
Crude protein	%	17.6	17.6
Crude fat	%	5.1	5.1
Crude fibre	%	5.0	5.0
Crude ash	%	3.5	11.8
Starch	%	37.5	29.3
Dextrin	%	15.7	15.7
Sugar	%	11.1	11.1
Calcium	%	0.55	0.55
Phosphorus	%	0.37	0.37
Magnesium	%	0.10	0.10
Energy	MJ/kg	15.7	14.4
Protein	kJ%	19	21
Fat	kj%	12	13
Carbohydrates	kJ%	69	66

At the conclusion of each dietary protocol, mice were anesthetized in the morning by intraperitoneal ketamine-xylazine injection. After mice reached the surgical plane of anaesthesia, blood was collected from the renal artery into heparin tubes. One hundred millilitres of whole blood were used to measure potassium and sodium electrolytes. The heart was isolated and dissected into the apex and the upper part. Apex was used for RNA isolation or protein analysis, while the rest was snap-frozen until further use. Minipumps were disposed of at the end of each experiment.

2.2. Osmotic minipumps preparation and implantation

The Ang II infusion experiment was conducted using osmotic pumps (ALZET 1004) with a release rate of 500 ng/kg/min during the 28 days. Each pump was filled completely with the Ang II powder dissolved in saline solution (Fresenius Kabi, Bad Homburg, Germany). When MRI measurements were to be performed, the metal tips were subsidised with PEEK (polyetheretherketone) tips. To prevent the cling of PEEK tips with Ang II, they were prewashed with 1 % Human Serum Albumin (HSA) in Phosphate buffer Dulbecco solution without Ca2+ and Mg 2+ (PBS). The prefilled pumps were incubated in sterile saline for 24 hours at 37°C to ensure an immediate release of Ang II upon implantation.

The subcutaneous implantation of osmotic minipumps took place in a sterile set-up. Mice were anesthetized with 1.5 % isoflurane or a mix of Ketamine (100 mg/kg, i.p.) and Xylazine (5 mg/kg, i.p.) and an ophthalmological cream was applied to the eyes of the mice. The implantation site in the neck was shaved and washed previously. An incision was made to create a subcutaneous pocket for the minipump placement. After the insertion, the wound was closed with sutures. The mice received 0.02 mL buprenorphine injection for pain relief and were closely monitored for the following days.

2.3. Implantation of spironolactone pellets

We blocked the MR by implanting spironolactone pellets, a dosage of 63 mg, with a release rate of up to 42 days. Mice were anesthetized with a mix of Ketamine (100 mg/kg, i.p.) and Xylazine (5 mg/kg, i.p.) and an ophthalmological cream was applied to the eyes of the mice. An incision was made in the lateral side of the neck, followed by a 2 cm pocket beyond the site. The pellet was inserted in the pocket and closed with sutures.

2.4. Blood pressure measurements

Systolic blood pressure was measured twice a week after the minipumps implantation in conscious mice by tail-cuff plethysmography (BP-98A; Softron) as described previously (Kurtz et al. 2005. Arterioscler Thromb Vasc Biol). The mice were placed in a restrainer equipped with a climatic coil to provide 37°C heating. The cuff was positioned at the proximal end of the tail of the mice. For habituation, mice were trained daily for 5 consecutive days before Ang II pump implantation. SBP was calculated as the mean of all measured values for each time per mouse.

2.5. MRI (Cardiac function)

To assess the cardiac function and cardiac anatomy of *Apoe*$^{-/-}$ mice, we performed ^{1}H magnetic resonance imaging (MRI) using a vertical 9.4 T Bruker AVANCE^{III} wide bore NMR spectrometer as described previously (Temme et al. 2021. Front Cardiovasc Med; Haberkorn et al. 2017. Circ Cardiovasc Imaging). Mice were anesthetized with 1.5% isoflurane at a rate of 75ml/min using a home-build nose cone. The body temperature (37^{o}C) was maintained throughout the whole measurement. For gated MRI acquisitions, the front-paws and the left hind-paw were attached to ECG electrodes (Klear-Trace) and respiration was monitored by means of a pneumatic pillow positioned at the animal's back. An M1025 system (SA Instruments, Stony Brook, NY) was utilized was utilized to monitor vital functions and, if needed, to synchronize the acquisition of cardiac MRI data with cardiac and respiratorymotion. Each measurement lasted 60-80 minutes. During a complete heart cycle, 15-20 images were acquired to gain temporal and spatial resolution for functional heart parameters determination. Images were acquired using the Bruker microimaging unit Micro 2.5 with actively shielded gradient sets (1.5 T/m) and a 25-mm birdcage resonator. The datasets were analysed with Fiji or in-house developed software-tools based on the Labview environment.

2.6. Metabolic cage experiments and urine measurements

Mice were placed in metabolic cages overnight at two different time points: before and after Ang II infusion. Food and water were available *ad libitum*. The urine samples were collected the next day, and a portion of 150 µL was used for potassium and sodium electrolyte analysis (Cobas 8000 ISE). The urinary aldosterone concentration was measured utilizing a competitive assay ELISA kit following the manufacturer's instructions. The assay ELISA kit is based on the competition between aldosterone and aldosterone tracer for a limited amount of Aldosterone Polyclonal Antiserum. The concentration of the Aldosterone Tracer is held constant to quantify how much aldosterone binds to the Aldosterone Polyclonal Antiserum. The plate has anti-rabbit IgG so that the antiserum can bind to it. 100 µL of each sample was added per well and assayed. The plate was covered with plastic film and incubated for 18 hours at 4ºC. Afterwards, the plate was washed, and the Ellman's Reagent (which contains the substrate to aldosterone tracer) was added to the well, resulting in an enzymatic reaction. The distinct yellow was determined spectrophotometrically, proportional to the amount of Aldosterone Tracer bound to the well, which inversely quantifies the aldosterone concentration in the well. The assay has a range from 15.6-2000 pg/ml.

2.7. Sirius red/Fast green staining

After dissection, the heart was placed in 10 % Formalin solution overnight for fixation. The next day, tissues were immersed in a serial dilution of ethanol, xylol and paraffin. Then, the tissues were embedded in paraffin blocks and stored at room temperature.

Formalin-fixed paraffin-embedded (FFPE) were cut using a sharp blade in 10 µm thick sections and placed over coated glass slides. To dewax the slides, initially, they were immersed in xylol for 10 minutes, followed by absolute ethanol twice, and then in 96 % ethanol, 80 % ethanol, and 70 % ethanol for 3 minutes each step. Lastly, the slides were washed in distilled water for 10 minutes.

Sirius Red/Fast Green collagen staining is a micro-assay used to determine collagen and non-collagenous proteins on tissue sections. The heart slides were incubated with one drop (0.2 - 0.3 ml) of staining kit solution for 30 minutes at room temperature and then rinsed with 0.5 ml distilled water. Afterwards, they were dehydrated and mounted (Roti©-Mount

HP68.1). Collagen fibers appeared red, while the non-collagen proteins were green. The quantitative analysis was obtained through microscopic images as a percentage of red pixels (the collagen) against green colour pixels (the non-collagen). The calculation was done by using Photoshop CS5.

2.8. Preparation of Cryo-conserved Tissues

After dissection, the heart was placed in 4 % PFA for 1 hour for fixation purposes. The fixed heart was immersed in 20% sucrose + PBS at 4°C for 2-3 hours. Afterwards, the tissue was placed into the freezing container and covered with TissueTek®, followed by overnight storage at -80°C. The heart sections were cut by using a cryotome.

Immunofluorescence Imaging

To visualize cardiac fibrosis, the heart slides were stained with Wheat Germ Agglutinin (WGA). Sections of hearts frozen were thawed for 20 minutes and re-hydrated in PBS for 5 minutes. The heart slides were incubated in blocking solution (0,1% saponin, 0.5% bovine serum albumin (BSA), 0,2% fish gelatine) for one hour at room temperature (RT) to prevent non-specific binding. Afterwards, the blocking solution was rinsed off by washing the slides in PBS for 3 sets of 3 minutes each. The primary antibodies (CD45, Ly6g, F4/80) were diluted in blocking solution and carefully applied onto the sections. The slides were then incubated overnight at 4°C in the dark. On the following day, the primary antibody was washed away by rinsing the slides in PBS for 3 sets of 3 minutes each. Subsequently, the secondary antibody was applied to the slides and incubated in the dark at RT for one hour. After another set of 3-minutes washes with PBS, the heart sections were stained using WGA for 1 hour in a dark chamber. After that, unbound WGA staining solution was removed with PBS (3 x 3 minutes) and slides were mounted using Prolong Diamond Antifade Mountant containing 4′,6-diamidino-2-phenylindole (DAPI), to stain live nuclei.

Senescence-Associated Beta-Gal Staining

To detect senescence presence in frozen tissue, β-Galactosidase Staining was performed as described previously (Jannone et al. 2020. J Histochem Cytochem). The tissue slides were rehydrated in PBS for 5 minutes and ready to be stained with the Senescence β-Galactosidase Staining Kit. The staining solution was made of X-Gal solution (25µL), staining buffer 10x (100 µL), Reagent B & C (12.5 µL) and distilled water (850 µL). Each heart section was

stained with 100 µL staining solution and incubated at 37ºC overnight. Next, the heart sections were washed with PBS and mounted. A bright field microscopy detected the blue staining representing the senescence and its location in the heart.

2.9. Flow cytometry-mitochondrial staining

Here, we describe how mitochondrial dyes are used to track mitochondrial content (as MitoTracker Green) and mitochondrial superoxide (as MitoSox Red) per different cardiac cell types using flow cytometry. The hearts were dissociated by combining mechanical dissociation with enzymatic degradation using the Multi Tissue Dissociation Kit 1 (0.5 g tissue in 2.5 ml enzyme mix). After 30 minutes of incubation at 37ºC, the mix was centrifuged, and the supernatant was discarded. Afterwards, the single cells were resuspended in MACS buffer and transferred to a 96-well round-bottom plate. We used the following panel to stain the cells:

- We diluted the anti-CD140a antibody 1/200 and mixed it with MitoTracker green (final 100nM) + MitoSox red (final 5 µM).
- We diluted the anti-CD31 antibody 1/200 and mixed it with MitoTracker green + MitoSox red, keeping the same final concentration.
- We diluted the anti-cTnT antibody 1/200 and mixed it with MitoTracker green + MitoSox red, keeping the same final concentration.
- Then, the cells were resuspended in antibody and probes mix (50 µL per well) and incubated for 15 minutes at 37ºC. Once the staining time was over, the cells were centrifuged (5 min at 1500 rpm and discarded supernatant) and resuspended in PBS + 2% FCS for acquisition in the flow cytometer.

We used flow cytometry to determine the mitochondrial ROS based on mitochondrial mass and production of superoxides. MitoTracker green is a probe that passively diffuses the membrane and accumulates in active mitochondria, representing the mitochondrial mass. MitoSox red is a live-cell permeant dye. It enters the mitochondria and is oxidized by superoxides, producing a strong red fluorescence (Excitation/emission wavelength: 396/610 nm). For this analysis, we considered the ratio of MitoSox against MitoTracker signal per cardiomyocytes, fibroblasts or endothelial cells. Flow cytometric measurements were done using Canto II™ Flow Cytometer (BD Biosciences, San Jose, USA). FlowJo v8 (FlowJo LLC) was used for data analysis.

2.10. Western blot analysis

Western blot is a technique used for protein detection, which includes denaturation and gel electrophoresis of the relevant samples. Adapted protocol according to (Quast et al. 2022. Basic Res Cardiol). Frozen heart (apex) tissues were minced in RIPA (radioimmunoprecipitation assay) lysate buffer (Table 2), and phosphatase and protease inhibitor. Then, the samples were homogenized by a Beadbug device using 1.5 mM zirconium bead-prefilled tubes. Detergents were added, and the homogenate was incubated for 1 hour with rotation at 4ºC. After 15 min of centrifugation at 15,000 g, the supernatant was collected for protein concentration determination using Bradford Reagent. To separate the proteins, sodium dodecyl sulfate polyacrylamide gel electrophoresis (SDS-PAGE) was used. After the separation, the proteins were transferred to nitrocellulose membranes. The blots were then stained with the Revert™700 Total Protein Stain and imaged with the LI-COR Odyssey Fc to confirm the protein loading. After destaining, the membranes were blocked for 1 hour with Intercept™ Blocking Buffer and incubated overnight at 4ºC with primary antibodies, diluted 1/1000 dilution in blocking buffer. The primary antibodies of interest used: OPA1-L Rabbit mAb, ATP5A1 Polyclonal Antibody, COX IV Rabbit Ab or Rabbit anti-LC3B pAb. After washing, the membranes were incubated with the secondary antibody Goat anti-Rabbit IgG (1/10.000 diluted in blocking buffer) for 1 hour at room temperature. After an additional washing, the membranes were imaged with the Odyssey Fc Imaging System within 700 and 800 nm. Integrated band intensity was quantified using Fiji software and normalized to the total protein staining using the Empiria Studio™ Software. The final results were presented as ratios.

Table 2. Buffer recipe.

Reagent	RIPA buffer
NaCl	150 mM
EDTA	5 mM
Tris	50 mM
Nonidet P40 substitute	1%
SDS	0.1 %
Sodium nitroprusside dihydrate	5%
dH_2O	84 ml

2.11. mRNA quantification and assessment by qPCR

qPCR stands for quantitative polymerase chain reaction, and it measures gene expression. RNA content was isolated using the RNeasy plus mini kit and following the manufacturer's instructions. The tissue was transferred to RLT buffer containing 10% β-merchaptoethanol and ruptured for 30 seconds. To eliminate the gDNA, the supernatant was placed in a gDNA column and centrifuged at 8000g briefly. After the discard of gDNA, 70% ethanol was added, and the mixture was transferred into an RNA column. To purify the RNA from carbohydrates, proteins or salts, the RNA column was twice with 350 µL RW1 buffer and 500 µL RPE buffer. To ensure total removal of gDNA, a DNAse enzyme was added to the column and incubated for 15 minutes. The column was centrifuged twice for 2 minutes at the maximum speed to remove any liquid. To obtain the purified RNA content, 50 µL of RNase free was placed in the column and centrifuged for 1 minute. The amount of RNA was quantified spectrophotometrically.

To obtain the complementary DNA (cDNA), QuantiTect Reverse Transcription kit was used. First, the isolated RNA of each sample was incubated with 2 µL gDNA wipe-out buffer at 42ºC for 2 minutes. A reverse-transcription master mix containing Quantiscript reverse transcriptase, Quantiscript RT and RT primer was prepared. 0.5 µL of each isolated RNA sample was mixed with the master mix and incubated at 95 ºC for minutes to acquire the cDNA.

As a final step, a master mix was made for quantitative RT-PCR. The master mix contained 10 µL /well sybr green, 0.1 µL/well reverse primer and 8.8 µL /well RNAse-free water. The master mix and 1 µL/well cDNA were pipetted into a 96-well plate. After sealing the plate, the qPCR process was performed by a 7300 Real-time PCR system (Thermofisher, Waltham, USA).

Table 3. The thermal cycles of qPCR.

Stage	Repetitions	Temperature	Time
1	1	95.0ºC	15:00
2	40	95.0ºC	00:15
		58.0ºC	00:30
		72.0ºC	00:30

		76.0°C	00:34
3 (Dissociation)	1	95.0°C	00:15
		60.0°C	01:00
		95.0°C	00:15
		60.0°C	00:15

The mRNA quantification was based on the fluorescence threshold (Threshold cycle, CT value). The CT value is the cycle of PCR at which the reporter fluorescence significantly exceeds background fluorescence, and a ΔC_t method was used to compare C_t values between groups. The expression of the target mRNA was normalized with the housekeeping gene GAPDH to calculate the relative expression of the mRNA.

qPCR Primers (Eurofins genomics, Germany) used were as the following:

- *Gapdh* (encoding Glyceraldehyde-3-phosphate dehydrogenase):
Forward: GTGTTCCTACCCCCAATGTGT
Reverse: GTCCTCAGTGTAGCCCAAGATG
- *Anp* (encoding Atrial natriuretic peptide):
Forward: CTGGGCTTCTTCCTCGTCTT
Reverse: CCTCATCTTCTACCGGCATCT
- *Bnp* (encoding Brain natriuretic peptide):
Forward: AAGGTGCTGTCCCAGATGATT
Reverse: CCATTTCCTCCGACTTTTCTC
- *Fn1* (encoding Fibronectin 1):
Forward: CGAGGTGACAGAGACCACAA
Reverse: CTGGAGTCAAGCCAGACACA
- βmhc: (encoding Beta- myosin heavy chain)
Forward: GGCAGAGCAGGACAACCTC
Reverse: AGGTCCGCGTTCACTTCCT
- *Col1a1* (encoding Collagen type 1 alpha 1 chain):
Forward: ATCTCCTGGTGCTGATGGAC
Reverse: ACCTTGTTTGCCAGGTTCAC
- Tnfα (encoding Tumor necrosis factor-alpha):
Forward: ATGTCTCAGCCTCTTCTCATTC
Reverse: GTCTGGGCCATAGAACTGATGA
- *Tgfβ1* (encoding Transforming growth factor beta 1)
Forward: GCTGCGCTTGCAGAGATTAAAA
Reverse: CGTCAAAAGACAGCCACTCA

- *Il-6* (encoding Interlekuin-6):
Forward: CAGAGGATACCACTCCCAACA
Reverse: GCCATTGCACAACTCTTTTCTC
- *Il-1*β (encoding Interleukin-1 beta):
Forward: GGATGAGGACATGAGCACCTT
Reverse: CTAATGGGAACGTCACACACC
- *Cdkn2a* (encoding Cyclin dependent kinase inhibitor 2a):
Forward: CTCGTGCTGATGCTACTGAGGA
Reverse: GGTCGGCGCAGTTGGGCTCC
- *Cdkn1a* (encoding Cyclin dependent kinase inhibitor 2a):
Forward: AGGTGGACCTGGAGACTCTCAG
Reverse: TCCTCTTGGAGAAGATCAGCCG

2.12. Statistical analyses

Data was curated in Microsoft Excel and analysed using Graph Pad Prism v9.4.1. For comparisons of more than two groups, data passing the Shapiro-Wilk normality test were assessed using one-way ANOVA (regular measurements) followed by SIDAK multiple comparison test. For repeated measurements, two- way ANOVA followed by TUKEY'S multiple comparisons test was used to compare two or more groups. For comparison of two groups at one time point, data meeting the Gaussian distribution assumption were assessed using an unpaired t-test. Two tailed t test was used to test for effects in any direction. One-tailed t test was used to detect a difference between the groups only in one direction. Data is plotted as mean ± standard error (SEM) alongside individual values from independent animals. Outliers were identified by ROUT test and excluded when necessary. The significant difference was considered when P value is <0.05 and it is represented by an asterisk (*).

2.13. List of materials

Name	Catalogue nr.	Brand, Company	Country
Aldosterone ELISA kit	501090	Cayman	Michigan, USA
Ang II	A9525-10MG	Sigma	Steinheim, Germany
ATP5A1 Polyclonal Ab	PA5-27504	Invitrogen	Massachusetts, USA
Bis-Tris 4-12% Gel	QP3510	SMOBIO	Hsinchu City, Taiwan
Bradford Reagent	ab119216	Abcam®	Cambridge, UK
CD140a Ab	323511	Biolegend	San Diego, USA
CD31 Ab	102423	Biolegend	San Diego, USA
cTNT Ab	130-120-403	Miltenyi	Cologne, Germany
COX IV Rabbit Ab	4844S	Cell Signalling	Boston, USA
DPBS	P04-37500	PAN Biotech	Aidenbach, Germany
EDTA	Calbiochem, Merck	Calbiochem, Merck	Darmstadt, Germany
Empiria Studio™ Software	Version 4	LI-COR	Nebraska, USA
Human Serum Albumin 1%		Albutein, Grifols	Frankfurt, Germany
Intercept™ Blocking Buffer	927-70001	LI-COR	Nebraska, Germany
Isoflurane	PZN-09714675	Piramal	Hallbergmoss, Germany
IRDye 800CW Goat anti-Rabbit IgG	926-32211	LI-COR	Nebraska, USA
K^+ diet (normal)	S3544-E042	SSNIF	Germany
K^+ diet (high)	S3544-E044	SSNIF	Germany
Ketamine	402082	Ketaset, Zoetis	New Jersey, USA

MitoSox	M36008	Invitrogen™	Massachusets, USA
MitoTracker	M7514	Invitrogen™	Massachusets, USA
Multi Tissue Dissociation Kit 1	130-095-927	Miltenyi Biotec Inc	California, USA
NaCl	3957.1	ROTH	Krlsruhe, Germany
Nitrocellulose Blotting membrane	10600003	Cytiva life sciences	Freiburg, Germany
Nonidet P40 Substitute	15875388	Honeywell Fluka™	New Jersey, USA
Odyssey Fc		LI-COR	Nebraska, USA
OPA 1 Rabbit mAb	80471S	Cell Signaling	Boston, USA
Osmotic pump	Model 1004	Alzet®, Durect	California, USA
PEEK tips	2612	Alzet, Durect	California, USA
Phosphatase Inhibitor Mini Tablets	A32957	Thermo Scientific	Massachusetts, USA
Rabbit anti-LC3B pAb	NB100-2220	NOVUSBIO	Clorado, USA
Revert™ 700 Distaining	926-11012	LI-COR	Nebraska, USA
Revert™ 700 TPS	926-11011	LI-COR	Nebraska, USA
Roti-Mount	HP68.1	ROTH	Karlsruhe, Germany
SDS 10%	A0676	AppliChem, ITW-Illinois Tool Works Inc.	Chicago, USA
Senesence β-Gal Staining kit	9860	Cell Signaling	Boston, USA
Sirius Red/Fast Green Staining kit	9046	Chondrex™	Washington, USA
Sodium nitroprusside dihydrate	ALX-400-001-G005	Alexis® Biochemicals, Enzo Biochem	New York, USA

Spironolactone pellets	SM-161	Innovative Research America	Florida, USA
TissueTek®	10225712	SAKURA	
Xylazine	3100265	Rompun, Bayer	Leverkusen, Germany

3. Results

To investigate the effect of high K^+ diet on cardiovascular health, *Apoe*$^{-/-}$ mice were treated with 5% potassium diet (high K^+) or 0.55 % potassium diet (normal K^+) throughout the whole experimental period. After two weeks of the diet start, osmotic minipumps filled with Ang II (500 ng/Kg/min) were implanted. At the end of the experiment, blood and urine samples were collected for potassium and aldosterone determination. One day before sacrifice, MRI was performed and mice were euthanized for cardiac function assessment.

3.1 High potassium diet does not affect Ang II-induced blood pressure

Mice fed a high K^+ diet for 42 days exhibited higher plasma potassium compared with mice fed a normal K^+ diet (5.9±0.4 vs 4.7±0.4 mmol/L, p<0.06). As expected, the excreted aldosterone in the urine was significantly higher for high K^+ mice both before and after Ang II infusion (Figure 8B). There was no significant difference before and after Ang II (213.9±72.4 vs 151.1±28.8 ng/24h, p<0.5). Baseline SBP was similar between both treatments (113±10 vs 116±4). Infusion of Ang II for four weeks resulted in a significant elevation of SBP to 161±7 and 171±13 mmHg for normal potassium treated and high potassium treated mice, respectively (Figure 9). However, no significant change was noted during the 4-weeks period between the diets.

Figure 8

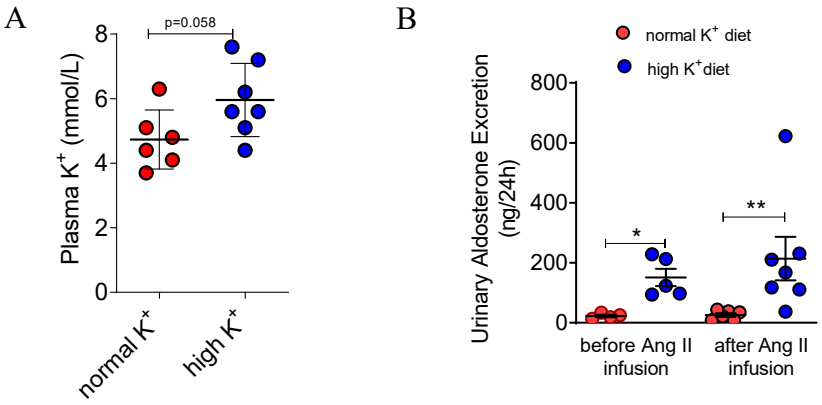

Fig.1: (A) Plasma potassium levels were higher in mice fed a high K^+ diet compared to mice fed a normal K^+ diet (5.9±0.4 vs. 4.7±0.4 mmol/L, P<0.058, n=6-7). (B) Urinary aldosterone excretion before Ang II, was significantly increased in the high K^+ group compared with the normal K^+ group (151.1±28.8 vs 22.5±4.4 ng/24h, *P<0.0059, n=4-5). 2-tailed t test was used to test differences.

Figure 9

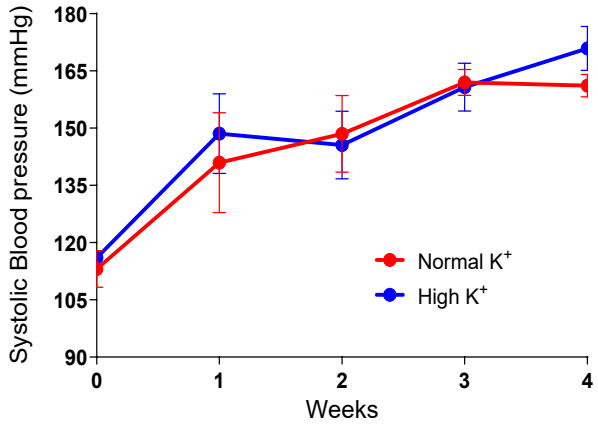

Fig. 9: Baseline SBP was similar between normal K^+ and high K^+ fed mice: (week 1, 141±26 vs 149 ±23 mmHg; week 2, 149±22 vs 146±20mmHg; week 3, 162±7 vs 161±14 mmHg; week 4, 161±7 vs 171±13 mmHg). Normal K^+ *Apoe*$^{-/-}$ Ang II n=5, High K^+ *Apoe*$^{-/-}$ Ang II n=5.

3.2. High potassium diet does not influence myocardial morphology and function in hypertensive mice

To evaluate the beneficial effect of high K^+ diet on cardiac outcome in Ang II infused mice, we noninvasively performed MRI measurements *in vivo* one day before the sacrifice. As shown in figure 10, there were no differences among parameters such as ejection fraction (EF), left ventricular mass (LVM), total ventricular mass (TVM), end systolic volume (ESV), end diastolic volume (EDV), diastolic wall thickness (DWT) and systolic wall thickness (SWT).

Figure 10

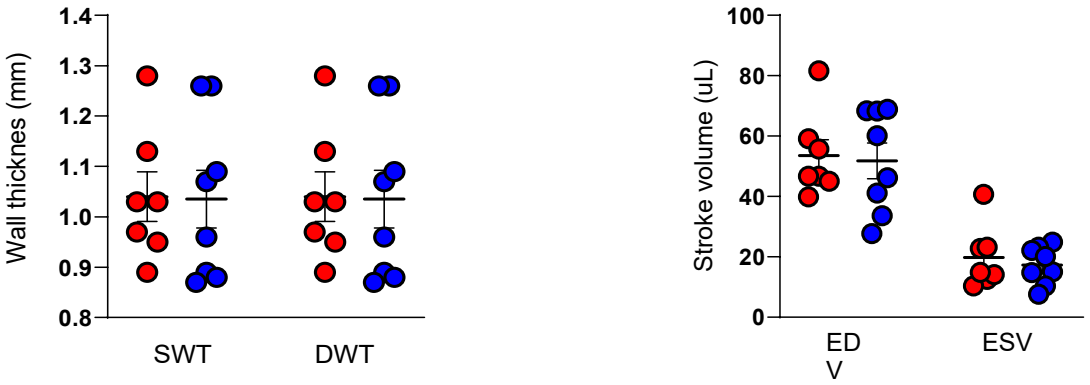

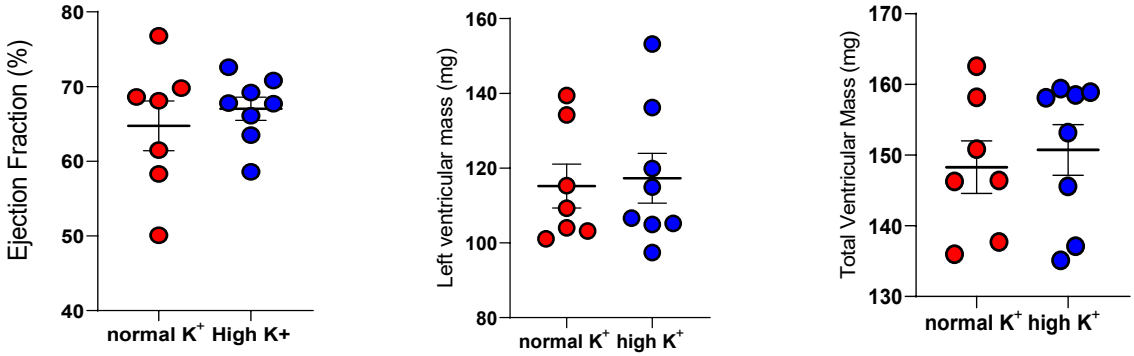

Fig.10: MRI parameters of cardiac function did not differ between the groups of Ang II infused mice (n=7-8): (normal K^+ vs high K^+: EDV, 53.5±5.3 vs 51.8±5.9 ul, P=0.8; ESV, 19.8±3.9 vs 17.3±2.2, P=0.6; LVM, 115±5.9 vs 117.3±6.6 mg, P=0.8; TVM, 148.3±3.7 vs 150.7±3.6 mg, P=0.6; EF, 64.7±3.3 vs 67.04±1.5 %, P=0.5). SWT and DWT were similar between normal K^+ and high K^+ fed mice respectively (1.04 vs 1.03 mm, P=0.9 and 1.04 vs 1.04, P=0.9). Two-tailed t-test was used for each parameter.

3.3. High potassium diet does not influence cardiac damage in hypertensive mice

In addition, relative mRNA expression of cardiac injury and fibrotic markers were assessed in the hearts of *Apoe*$^{-/-}$ mice. The relative expression of ANP was significantly lower in the high K^+ group compared to the control group, as shown in figure 11A. Whereas, no difference was observed for BNP and β-MHC, collagen and fibronectin. Cardiac tissue of the mice was stained for fibrosis and the Sirius red/Fast green analysis revealed that mice fed a high potassium or control diet produce similar collagen content (figure 12). In summary, the present results suggest that high potassium diet has no effect on myocardial morphology and function.

Figure 11

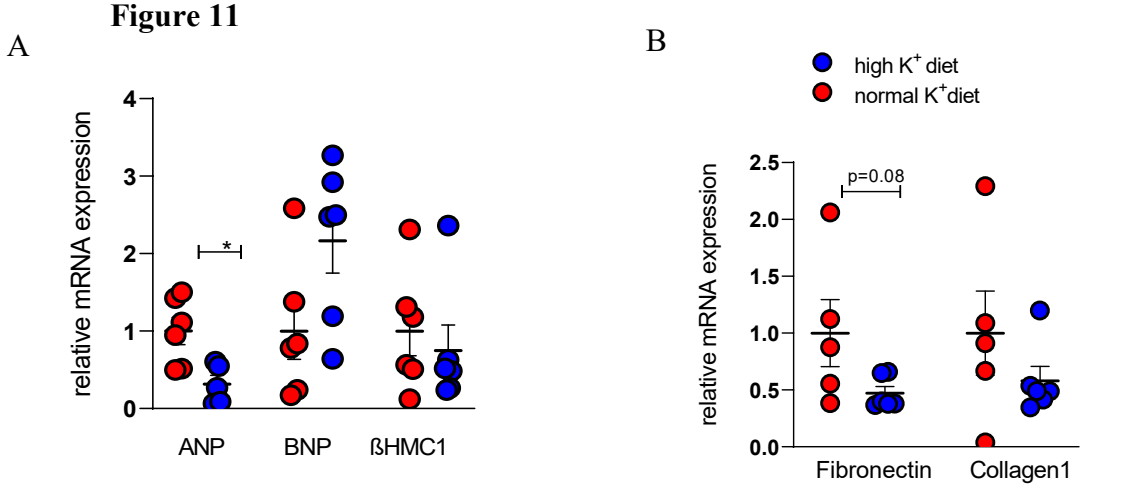

Fig.11: (A) High potassium fed mice had lower expression of cardiac ANP [explain] relative to normal potassium group (0.3±0.2 vs 1±0.6 mRNA, *P<0.01, n=5). Relative expression of BNP (1±0.3 vs 2.1±0.4 mRNA, P=0.06, n=5-6) and β-MHC (1±0.3 vs 0.7±0.3, P=0.6, n=6). High K^+ diet increases the relative expression of fibronectin compared to normal K^+, although not significantly (1±0.3 vs 0.5±0.1 mRNA, P=0.08, n=5-6). Collagen expression in the hearts of high and normal K^+ diet was similar.

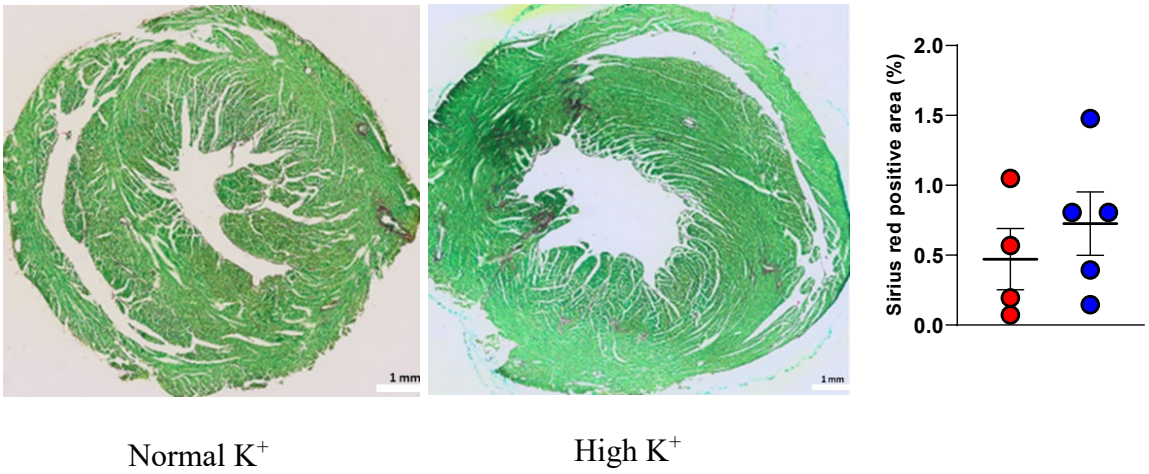

Fig.12: The collagen content in the hearts of Ang II infused mice was assessed by Sirius Red/Fast Green staining and analysed as a ratio between collagen to non-collagen part (n=4-5). Collagen content did not differ between the two groups (0.5±0.2 vs 0.7±0.2, P=0.5). Two-tailed t test was used for the comparisons.

To evaluate the consequence of potassium mediated aldosterone secretion for hypertensive cardiovascular damage, we additionally treated our high K^+ groups with 1% Na^+ (Figure 13). High sodium has been shown to aggravate the aldosterone effects on the cardiovascular system.

Figure 13

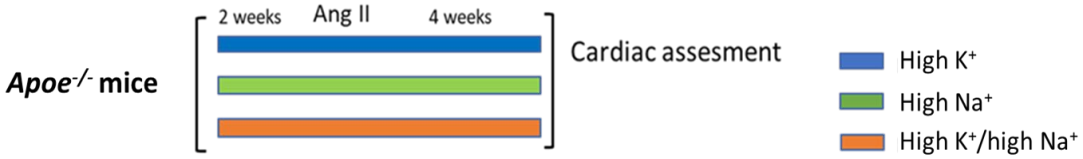

3.4. The combination of chronic high potassium/high sodium diet aggravates Ang II-induced hypertension

To determine the effect of the added high Na^+ to high K^+ intake on SBP, mice were fed with the following diets: High K^+ diet (5%), high Na^+ in the drinking water (1%), high K^+ diet and high Na^+ in drinking water concomitantly for six weeks. At baseline SBP was similar among the diets. Ang II infusion elevated the BP values by 25mmHg in the first week. The SBP increased constantly during the 2^{nd} and 3^{rd} week of Ang II infusion, but without a significant difference between the three groups. At week 4 of Ang II infusion, SBP was significantly higher in mice fed a high K^+/high Na^+ compared to mice fed a high K^+ diet (164±5 vs 141±6 mmHg, $p<0.02$). SBP was also elevated in high Na^+ treated mice (155±5 mmHg), although trending, it was not significant compared to high K^+ fed mice. These results suggest that elevated blood pressure is mainly driven by high sodium.

Figure 14

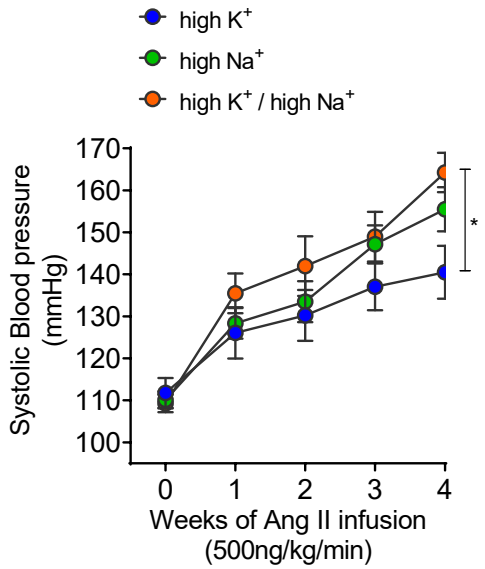

Fig.14: All treated mice showed similar baseline SBP values (108.6 vs 110.1 vs 111.8 mmHg, P=0.8). During the 3-week chronic Ang II infusion, SBP responses were not significantly different between the diets (high K^+/high Na^+ vs high K^+ vs high Na^+: week 1, 136±5 vs 126±6 vs 128±4 mmHg; week 2, 142±7 vs 133±5 vs 130.2±6 mmHg; week 3, 149±6 vs 147±5 vs 137±6 mmHg). There was observed an increase of SBP in high K^+/high Na^+ fed mice compared to high K^+-fed mice 164±5 vs 141±6 mmHg on the 4th week, *P<0.02 by two-way ANOVA. High K^+/high Na^+ *Apoe*$^{-/-}$ Ang II n=12, High K^+ *Apoe* $^{-/-}$ Ang II n=9, High Na^+ *Apoe*$^{-/-}$ Ang II n=10.

3.4. Effect of high potassium/high sodium on blood and urinary excretion of Na+, K+ and aldosterone

Plasma potassium concentration from the sacrifice day did not differ among the groups as shown in figure 15 B. Plasma sodium concentration was significantly higher in mice fed a high K^+/high Na^+ or high Na^+ compared to high K^+ diet alone (148.3±0.7 vs 141.2±0.6 and 147.9±0.3 vs 141.2±0.3 mmol/L, p<0.0001). To gain more insights, we measured urinary parameters associated with high blood pressure. The urinary potassium excretion was significantly higher in the Ang II infused mice fed high K^+ or high K^+/high Na^+ diet compared to high Na^+-fed animals. As predicted, the same mice excreted more aldosterone compared to high Na^+-fed mice (116.5±26.8 vs 25.7±6.3 and 74.4±11.4 vs 25.7±6.3 ng/24h, p<0.001). Total urinary aldosterone excretion of high K^+/high Na^+ treated mice after Ang II was significantly higher compared to pre-Ang II infusion (74.4±11.3 vs 39.20±7.6 ng/24h, p<0.02). Notably, mice fed a high K^+/high Na^+ diet excreted higher amount of sodium compared to high K^+ or high Na^+ treated mice, indicating a potential natriuretic role of potassium (42.7±9.9 vs 2.96±0.6 and 42.7±9.9 vs 10.8±2.5 mg/24h, p<0.002).

Figure 15

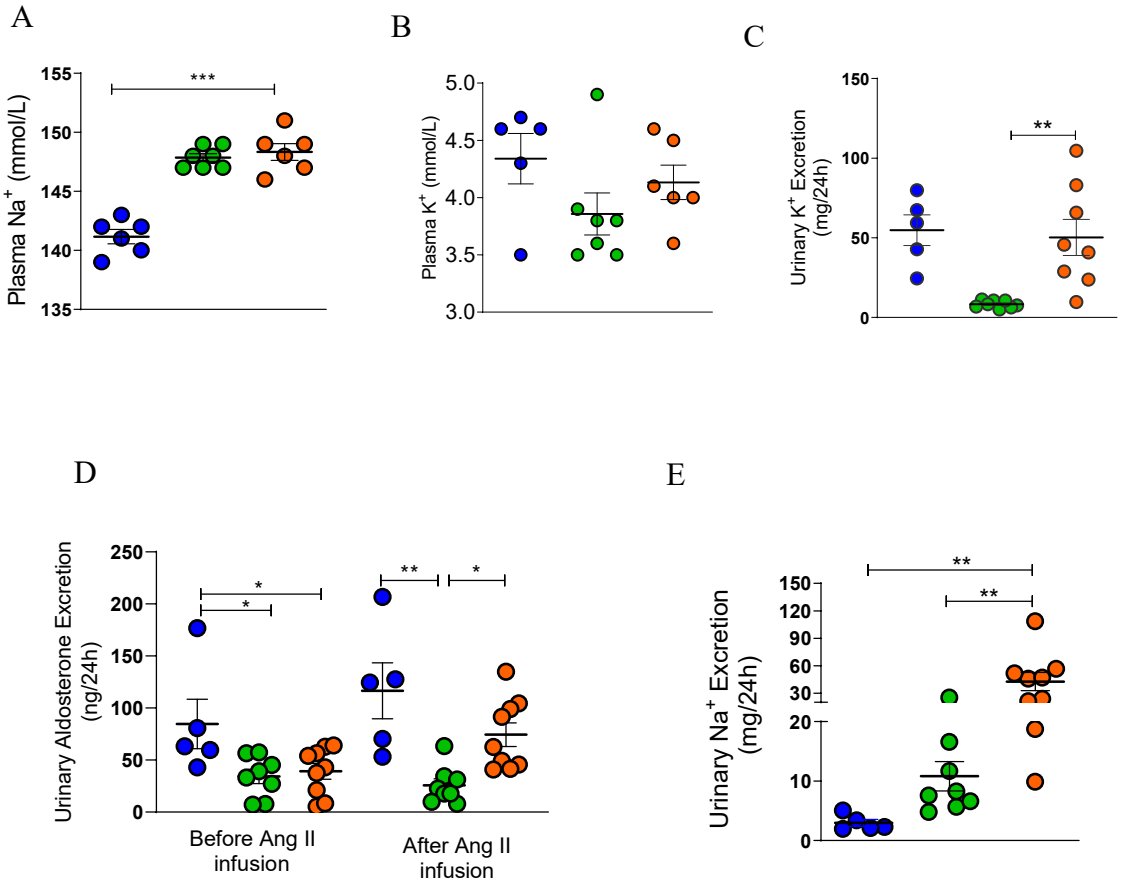

Fig. 15: (A) Ang II infused mice fed a high K^+/high Na^+ (n=6) and high Na^+ (n=7) diet exhibited higher plasma sodium concentration compared to mice fed a high K^+ (n=6) diet (148.3±0.7 vs 141.2±0.6 and 147.9±0.3 vs 141.2±0.3 mmol/L, **** P<0.0001). (B) No differences in plasma potassium were detected. (C) 4 weeks after Ang II infusion, urinary potassium excretion rates were significantly higher in mice fed a high K^+ (n=5) and high K^+/high Na^+ diet (n=8) compared to high Na^+ diet (n=8) (54.7±9.7 vs 8.3±0.8 and 50.3±11.3 vs 8.3±0.8 mg/24h, **P <0.002). (D) High K^+ (n=5) increased significantly the urinary aldosterone excretion rate before Ang II, compared to high Na^+ (n=8) or high K^+/high Na^+ (n=9) diet in mice (84.7±23.7 vs 34.3±6.9 and 84.7±23.7 vs 39.2±7.6 ng/24h, *P<0.02). During Ang II infusion, urinary aldosterone excretion was significantly elevated in mice fed a high K^+ and high K^+/high Na^+ diet compared to high Na^+ diet (116.5±26.8 vs 25.7±6.3 and 74.4±11.4 vs 25.7±6.3 ng/24h, **P<0.0013). (E) Urinary sodium excretion, measured after Ang II infusion was significantly increased in mice fed a high K^+/high Na^+ diet compared to high K^+ or high Na^+ fed mice (42.7±9.9 vs 2.96±0.6 and 42.7±9.9 vs 10.8±2.5 mg/24h. **P<0.002). One-way ANOVA followed by TUKEY'S multiple comparisons was used as a test per each graph.

3.5. High potassium/high sodium induces cardiac hypertrophy

To determine the effect of high Na^+ diet on cardiac hypertrophy, heart to body weight and heart weight to tibia length index were evaluated at the time of sacrifice. We observed that Ang II-infused *Apoe*$^{-/-}$ mice fed a high K^+/high Na^+ diet developed more cardiac hypertrophy compared to high K^+ or high Na^+-fed mice. The observation was verified by performing MRI measurements at the end of the experimental period. The MRI revealed that left ventricular mass was significantly greater in mice fed high K^+/high Na^+ compared to mice treated with high Na^+ (150.9±6.6 vs 123.1±5.1 mg, $p<0.005$) (Figure 17A). There was no change in total ventricular mass parameter. High K^+/high Na^+-fed mice had an increased diastolic wall thickness (1.1±0.03 vs 0.95±0.03 mm, $p<0.01$), whereas the systolic wall thickness was similar among the treatments (Figure 17E, F). No difference was found in end systolic volume and end diastolic volume in any of the three groups. The ejection fraction was reduced down to 54% in mice fed a high K^+/high Na^+ diet, although it was not significantly lower compared to high K^+ or high Na^+-fed mice (Figure 17H). These observations point to higher chance of developing heart failure with preserved ejection fraction when supplied with high potassium and high sodium concomitantly in Ang II infused mice.

Figure 16

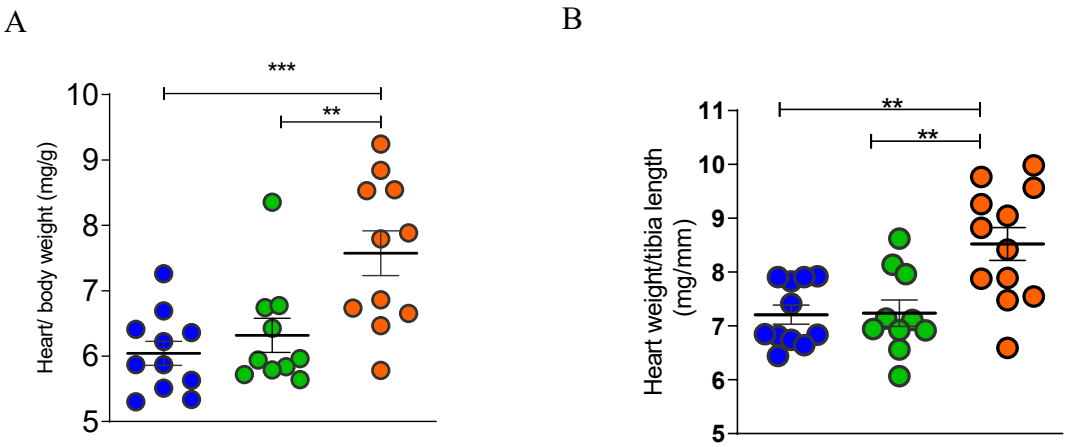

Fig.16: (A, B) Heart to body weight ratio and heart to tibia length ratio was significantly higher in high K^+/high Na^+ group in comparison to the high K^+ or high Na^+ group, respectively (7.6±0.3 vs 6.04±0.2 and 7.6±0.3 vs 6.3±0.3 mg/g), ***$p < 0.0008$, n= 10-11) (8.5±0.3 vs 7.2±0.2 and 8.5±0.3 vs 7.2±0.4 mg/mm, ***$P<0.0008$, n=10-11). One-way ANOVA followed by SIDAK'S multiple comparisons was used to test the differences.

Figure 17

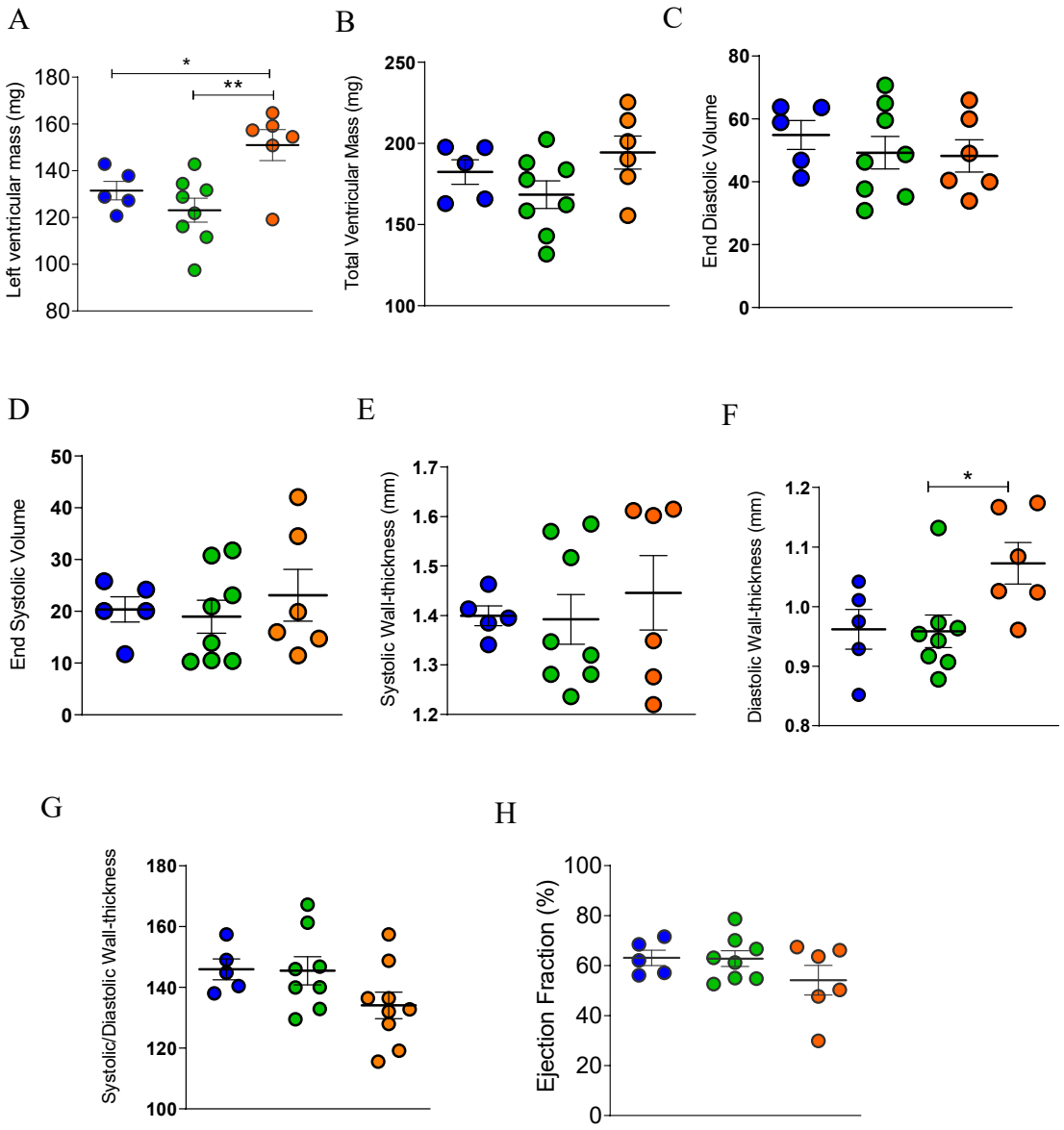

Fig.17: (A) LVM is increased in high K^+/high Na^+ fed mice (n=6) compared to high K^+ (150.9±6.6 vs 131.5±3.9, P=0.06, n=5) and high Na^+ treated mice (150.9±6.6 vs 123.1±5.1mg, **P<0.0019, n=8). (B, C, D, E) The following MRI parameters of cardiac function did not differ between the groups of Ang II infused mice: (high K^+/high Na^+ vs high K^+ vs high Na^+: TVM, 194.4±10.2 vs 182.4±7.5 vs 168.4±8.5 mg, P=0.13; EDV, 48.2±5.1 vs 54.8±4.6 vs 49.3±5.2 ul, P=0.6; ESV, 23.1±5 vs 20.4±2.4 vs 18.96±3.1 ul, P= 0.7; SWT, 1.4±0.07 vs 1.4±0.005 vs 1.4±0.02 mm, P=0.76). (F) DWT was higher in high K^+/high Na^+ fed mice compared to high Na^+ (1.1±0.03 vs 0.95±0.03 mm, *P<0.01) and high K^+ group (1.1±0.03 vs 0.96±0.02 mm, P=0.07). (H) Ejection fraction was reduced in high K^+/high Na^+ relative to high K^+ or high Na^+- fed mice (54.2±5.9 vs 63.1±3.04 and 54.2±5.9 vs 62.8±3.1 %, P=0.3). One-way ANOVA followed by SIDAK'S comparisons was used for all MRI parameters.

3.6. High potassium/high sodium drives cardiac fibrosis accompanied by senescence

One of the main causes for hypertension-mediated cardiac damage is fibrosis. Thus, we subsequently assessed fibrosis in the hearts of Ang II infused mice. High K^+/high Na^+ diet increased significantly the cardiac collagen production in Ang II infused mice compared to high Na^+ diet (1.5±0.3 vs 0.4±0.1 %, $p<0.02$) (Figure 18). To validate the IHC results, relative mRNA expression of markers characterizing fibrosis was measured in the cardiac tissue of hypertensive *Apoe*$^{-/-}$ mice. The mRNA of collagen1 and fibronectin was significantly higher in high K^+/high Na^+ fed mice compared to high K^+ or high Na^+ treated mice. For illustrative purposes (Figure 20), cardiac histologic sections of one mouse per treatment, were stained for cardiomyocytes-red, WGA - green and fibroblasts-blue. Hypertensive *Apoe*$^{-/-}$ mice fed with high K^+ diet showed no fibrosis (figure 20 A). High Na^+ murine heart displays a perivascular fibrotic phenotype (figure 20 E). Whereas the mouse fed with high K^+/high Na^+ developed extensive fibrosis in multiple cardiac regions. Fibrosis has been associated with cellular senescence, and persistent cardiac fibroblast senescence has shown to be deleterious (Osorio et al. 2023. Molecular Basis of Disease). Therefore, the same histologic sections of the heart were co-stained for Senescence-Associated-β-galactosidase (SA-β-gal) activity. The IHC illustrated that the same fibrotic regions of the high K^+/high Na^+ myocardium are accompanied with SA-β-gal (figure 20 L). Likewise, high Na^+ induces perivascular fibrosis accompanied with senescence in the murine heart (figure 20 H). Additionally, senescence mediators including p16 and p21 genes were evaluated. High K^+/high Na^+ treated hearts are shown to have higher expression of mRNA p16 and p21 in comparison to high K^+ or high Na^+ treated ones (figure 19 C, D). Overall, an exaggerated fibrotic effect of the combination of the diet in Ang II infused mice resulted in premature cellular senescence.

Figure 18

A

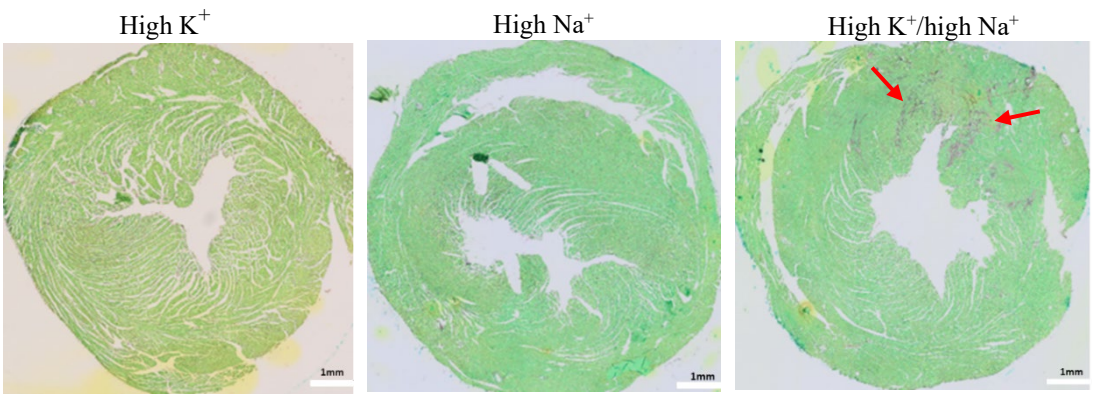

B

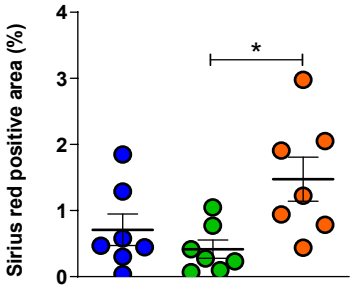

Fig.18: (A & B) Representative pictures of Sirius red/Fast green stained cardiac tissue. Quantification of collagen content to non-collagen area revealed that high K^+/high Na^+ -fed mice have more collagen compared to high Na^+ fed mice (1.5±0.3 vs 0.4±0.1 %, *P<0.04 n=7) by one-way ANOVA followed by SIDAK'S multiple comparisons test.

Figure 19

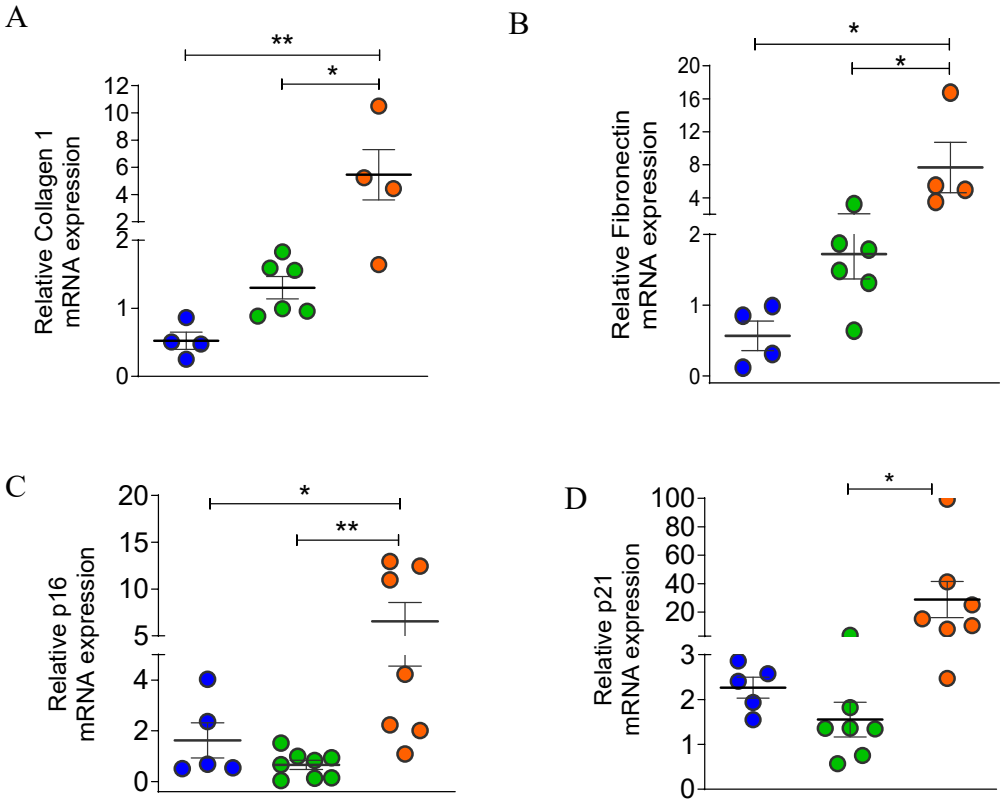

Fig.19: (A, B) High K^+/high Na^+ diet significantly increased the Collagen 1 expression relative to high K^+ or high Na^+ diet in Ang II *ApoE*$^{-/-}$ mice (5.5±1.8 vs 0.5±0.1 and 5.5±1.8 vs 1.3±0.2 mRNA, **P<0.008, n=4-6). Fibronectin mRNA expression was significantly higher in high K^+/high Na^+-fed mice (n=4) compared to high K^+ (n=4) or high Na^+ (n=6) fed mice (7.7±3.1 vs 0.6±0.2 and 7.7±3.1 vs 1.7±0.4 mRNA, *P<0.01). (C, D) Cardiac p16 and p21 mRNA expression was significantly increased in mice fed a high K^+/high Na^+ (n=7) diet compared to mice fed a high K^+ (n=5) or high Na^+ (n=8) diet (6.6±2 vs 1.6±0.7 and 6.6±2 vs 0.7±0.2 mRNA, **P<0.007) (28.8±12.7 vs 2.3±0.2 and 28.8±12.7 vs 1.5±0.4 mRNA, *P<0.04). One-way ANOVA followed by SIDAK'S multiple comparison test.

Figure 20

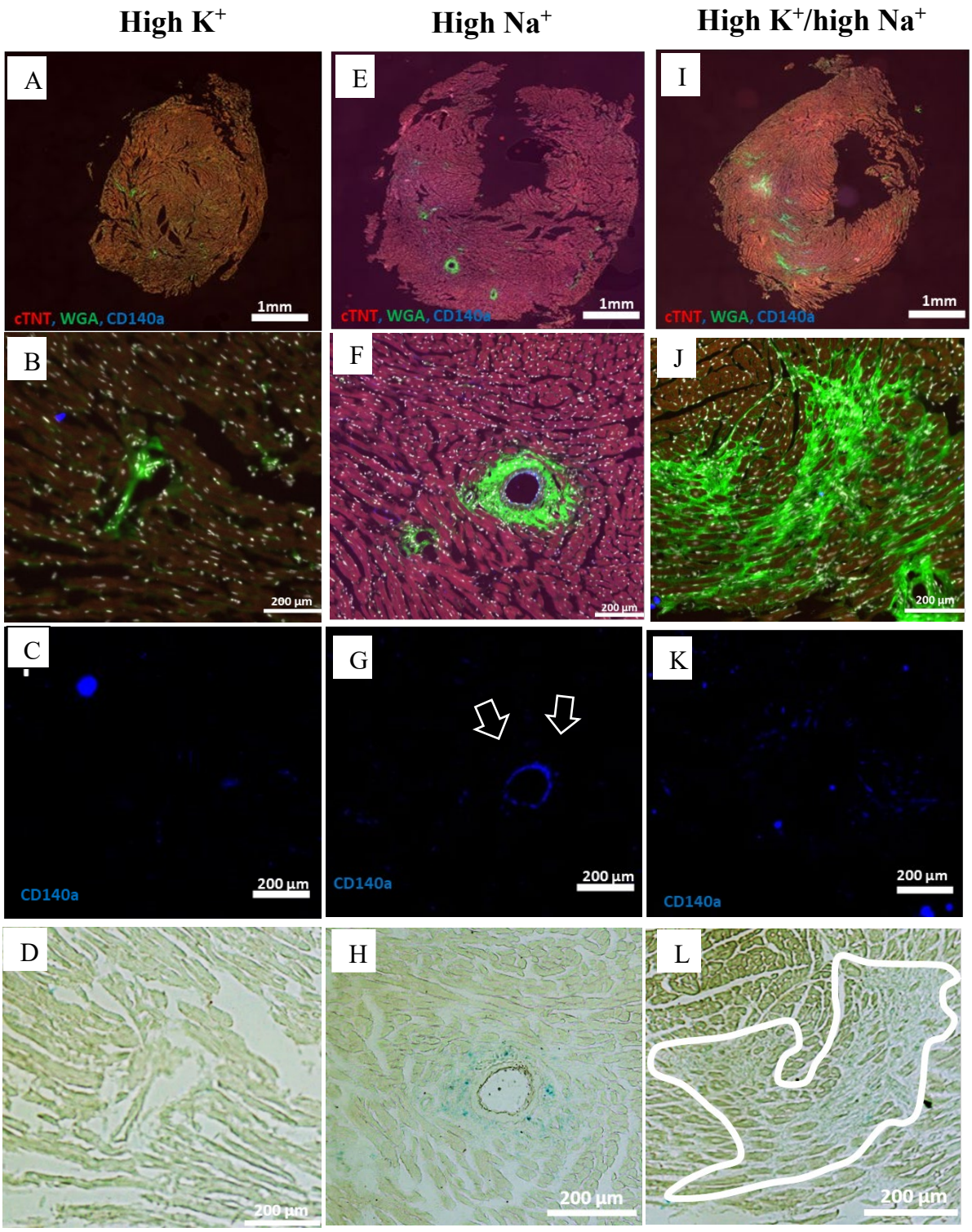

Fig.20: (A, B, C, D) Representative pictures of cardiac histologic section of high K^+-fed mouse. (E, F, G, H) Representative pictures of cardiac histologic section of high Na^+-fed mouse. (I, J, K, L) Representative pictures of cardiac histologic section of high K^+/high Na^+ fed mouse. cTnT-cardiomyocytes, WGA-Wheat Germ Agglutinin, CD140a-fibroblasts.

3.7. High potassium/high sodium accelerates cardiac inflammation

Given that inflammation is one of the main triggers of cardiac fibrosis and senescent cells are known to express high levels of pro-inflammatory factors, we analyzed the relative expression of different inflammatory cytokines. Mice fed a high potassium diet or high K^+/high Na^+ had an increased expression of MCP1 compared to high Na^+. The relative expression of the pro-inflammatory cytokines and profibrotic and endothelial stress factors- TNFα, IL-6, IL-1β, TGFβ and iNOS was significantly higher in the hearts of high K^+/high Na^+ treated group compared to the high K^+ or high Na^+ treated group (Figure 21). Moreover, we found a positive correlation between senescence marker p21 and the inflammatory cytokine IL-6 (R=0, P=0.007) in the high K^+/high Na^+ treated group (Figure 22), an indicator of SASP.

Figure 21

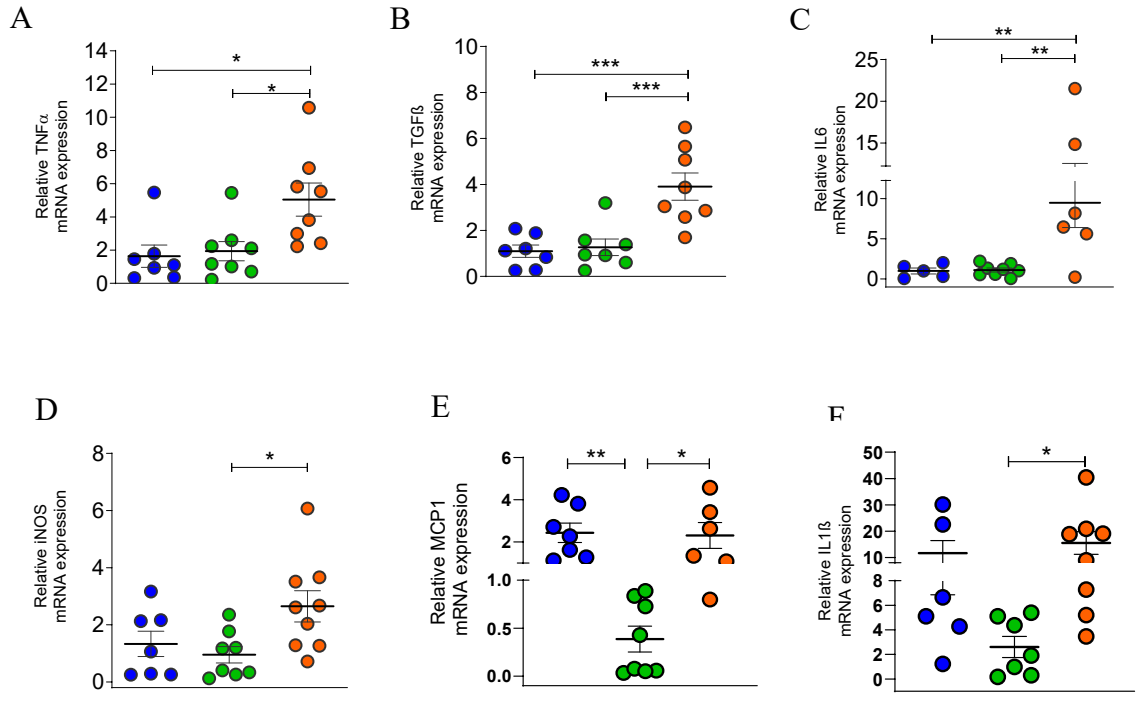

Fig.21: (A,B,C,D) Ang II *Apoe*$^{-/-}$ mice fed a high K^+/high Na^+ diet had higher relative expression of pro-inflammatory, fibrotic and endothelial stress factors compared to high K^+ or high Na^+ fed mice: (TNFα, 5.04±0.9 vs 1.6±0.7 and 5.04±0.9 vs 1.9±0.6 mRNA, **P<0.009, n=7-8; TGFβ, 3.9±0.6 vs 1.1±0.7 and 3.9±0.6 vs 1.3±0.4 mRNA, ***P<0.0003, n=7-8; IL6, 9.5±3.1 vs 1±0.4 and 9.5±3.1 vs 1.1±0.3 mRNA, **P<0.003, n=5-7; iNOS, 2.6±0.5 vs 1.3±0.4 and 2.6±0.5 vs 0.9±0.3, *P<0.03, n=7-8). (E) IL1β relative expression was higher in mice fed high K^+/high Na^+ compared to mice fed a high Na^+ diet (15.5±4.3 vs 2.6±0.8 mRNA, P=0.06). (F) MCP1 relative expression was significantly increased in mice fed a high K^+ or high K^+/high Na^+ diet compared to high Na^+ fed mice (0.4±0.1 vs 2.4±0.5 and 0.4±0.1 vs 2.3±0.6 mRNA, **P<0.003, n=7-8). One -way ANOVA followed by SIDAK'S multiple comparisons test.

Figure 22

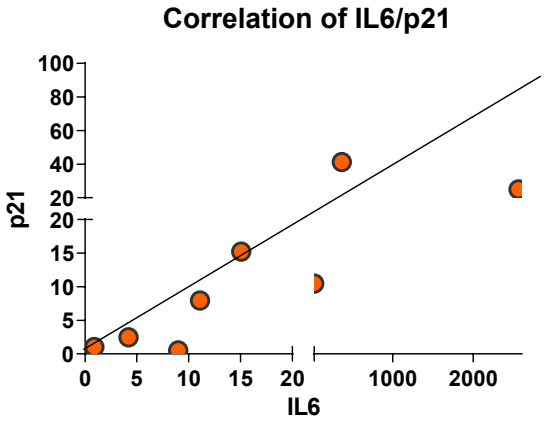

Fig.22: Plotting the relative mRNA expression of IL-6 against p21 in hearts from high K^+/high Na^+ fed mice, revealed a positive correlation P=0.007 and R=0.8, n=8.

3.8. High potassium/high sodium induces mitochondrial ROS in specific cardiac cell types

Senescence is associated not only with p21 expression and SASP markers but also with mitochondrial ROS production. We wanted to acquire a clearer appreciation of which cardiac cell type contributes to mitochondrial ROS, therefore we co-stained cell suspensions of the heart for fibroblasts (CD140a+), cardiomyocytes (cTnT+), endothelial cells (CD31) and measured mitochondrial ROS in correlation with mitochondrial mass (MitoSox/MitoTracker). We evaluated the ratio of Mitochondrial ROS/Total ROS to gauge the produced amount of ROS from different cardiac cells (Figure 24). The samples were normalized to the MT/MS signal in lean mice of 12 weeks without diet in each baseline experiment. Flow cytometry analysis revealed that fibroblasts (CD140a+) of high K^+/high Na^+ treated hearts produce significantly higher mitochondrial ROS amount relative to high K^+ or high Na^+ (181±9.7 vs 131±8.5 and 181±9.7 vs 136.6±10.7, **p<0.05). Cardiomyocytes (cTnT+) of high K^+/high Na^+ fed mice have significantly higher rates of ROS compared to high K^+ fed mice (182.1±15.8 vs 130.3±9.9, p<0.04). High Na^+ treatment elevated the endothelial cells ROS levels compared to high K^+/high Na^+ or high K^+ alone, although not significantly. This suggests that the senescence is mediated mainly by mitochondrial ROS of fibroblasts in mice fed a high potassium and high salt diet.

Figure 23

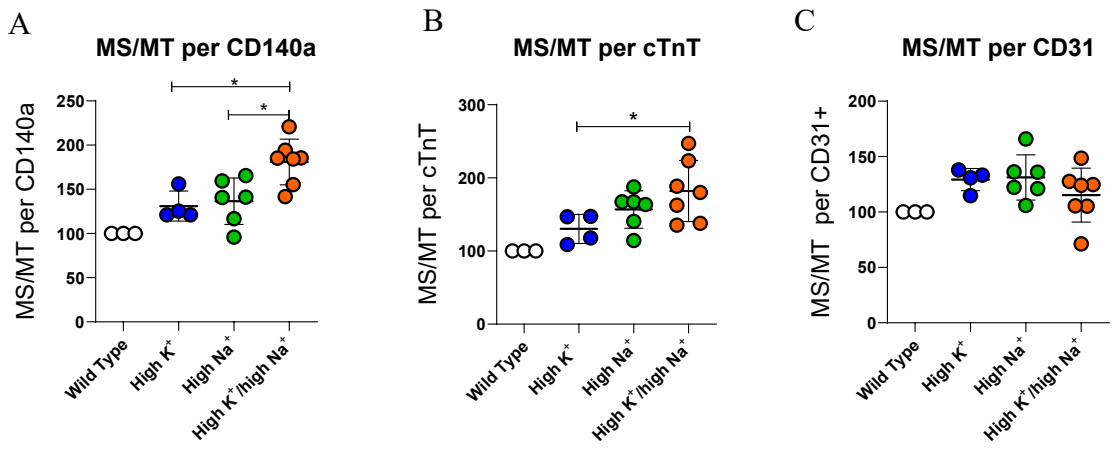

Fig.23: (A) Cardiac fibroblasts of high K^+/high Na^+ fed mice stained for mitochondrial ROS exhibited an increased MS/MT ratio compared to cardiac fibroblasts of mice fed a high K^+ or high Na^+ diet (181±9.7 vs 131±8.5 and 181±9.7 vs 136.6±10.7, **P<0.05). (B) MS/MT ratio per cardiomyocytes was higher in high K^+/high Na^+ -fed mice compared to high K^+ or high Na^+ fed mice (182.1±15.8 vs 130.3±9.9 and 182.1±15.8 vs 156.9±10.5, *P<0.04). (C) MS/MT ratio per endothelial cells did not differ among the three groups: (high K^+/high Na^+ vs high K^+ and high K^+/high Na^+ vs high Na^+; 115.3±9.2 vs 129.2±5 and 115.3±9.2 vs 131.2±8.3, P=0.4). High K^+/high Na^+ *Apoe*$^{-/-}$ Ang II n=7, High K^+ *Apoe*$^{-/-}$ Ang II n=4, High Na^+ *Apoe* $^{-/-}$ Ang II n=6. One-way ANOVA followed by SIDAK'S multiple comparisons test.

Figure 24

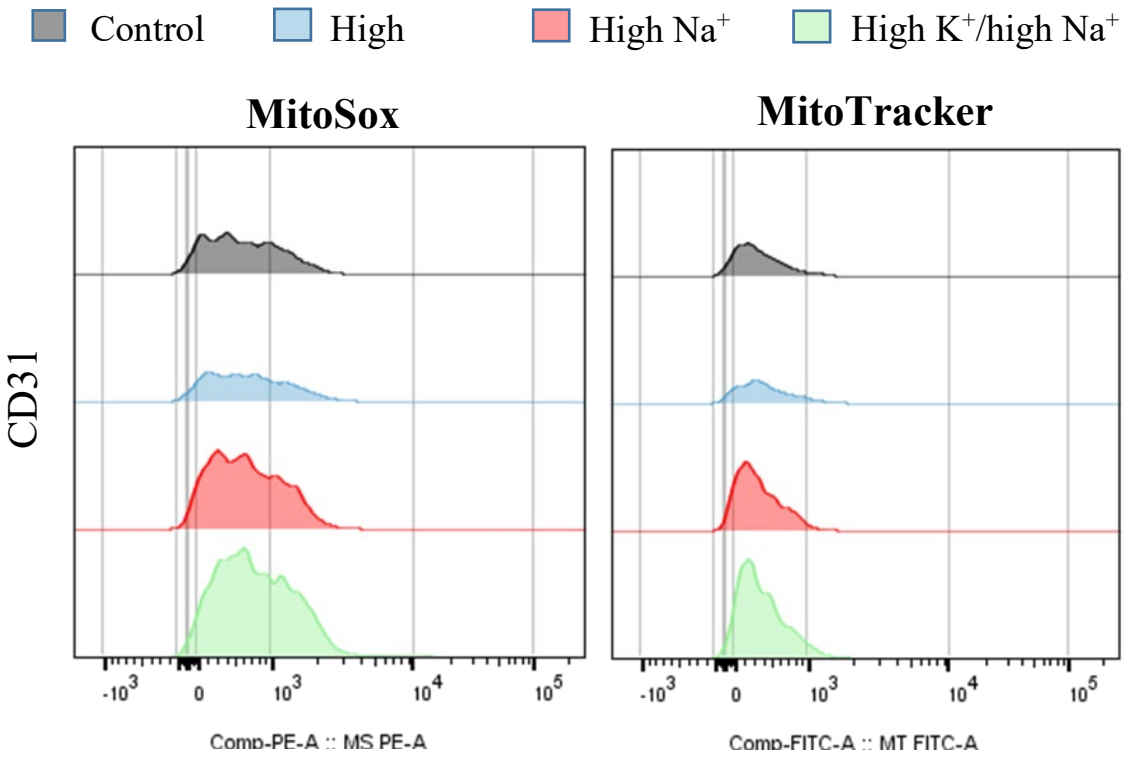

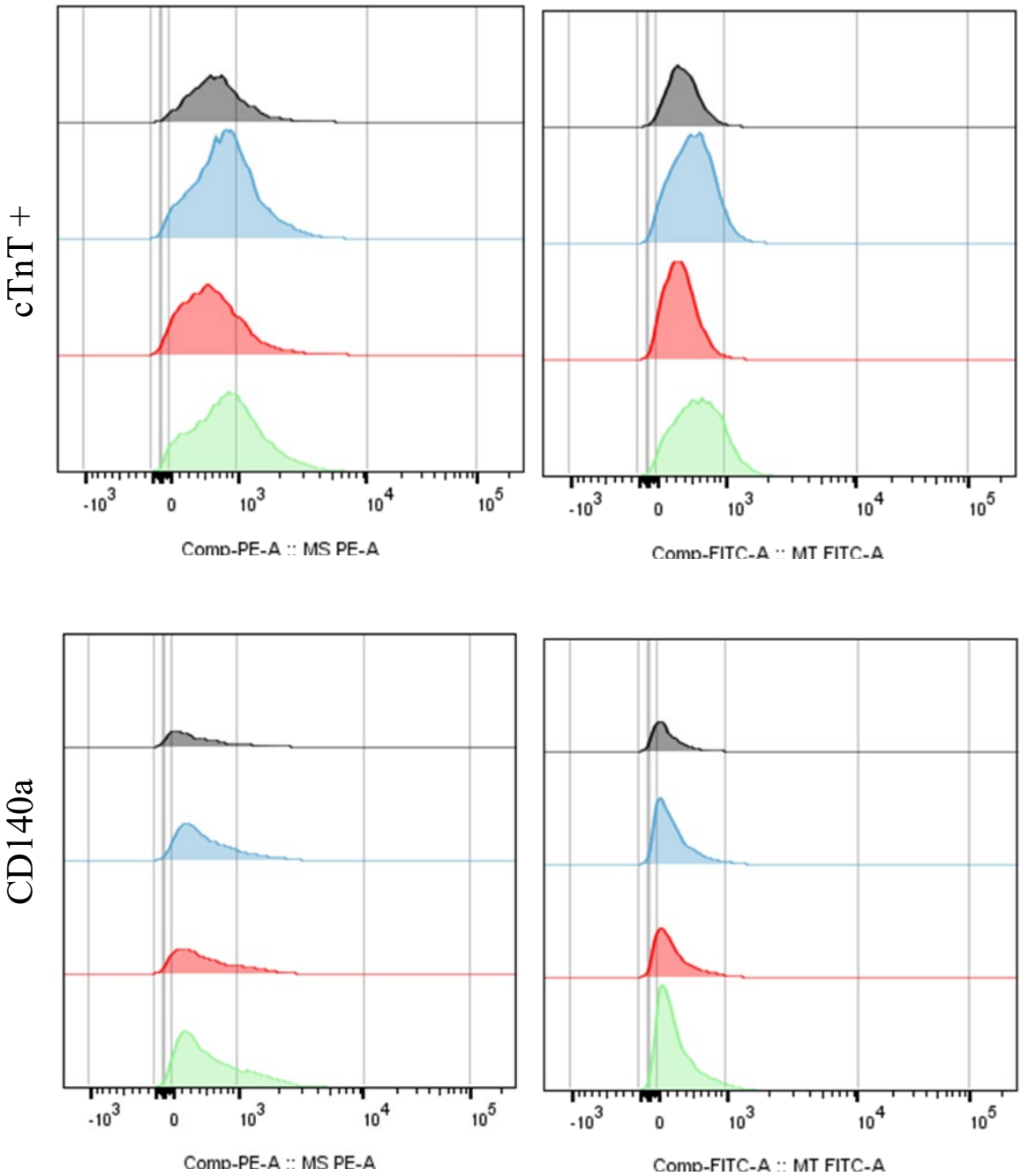

Fig.24: Representative Histograms of MitoSox and MitoTracker signal per each cardiac cell. CD31- endothelial cells, CD140a-fibroblasts, cTNT- cardiomyocytes.

3.9. Is potassium-induced aldosterone secretion in the setting of high sodium the main trigger for cardiovascular damage?

To investigate whether potassium-induced aldosterone secretion in the setting of high sodium is the main trigger of cardiac damage, we blocked the mineralocorticoid receptor (MR) to inhibit the actions of aldosterone. High potassium/high sodium fed mice were treated with spironolactone for 6 weeks (figure 25). To validate the MR blockade; urinary aldosterone excretion was measured at the end of the experimental period. High K+/high Na^+ fed mice treated with spironolactone had higher aldosterone excretion compared to non-treated spironolactone high K^+/high Na^+ fed mice (Figure 25B).

Figure 25

A

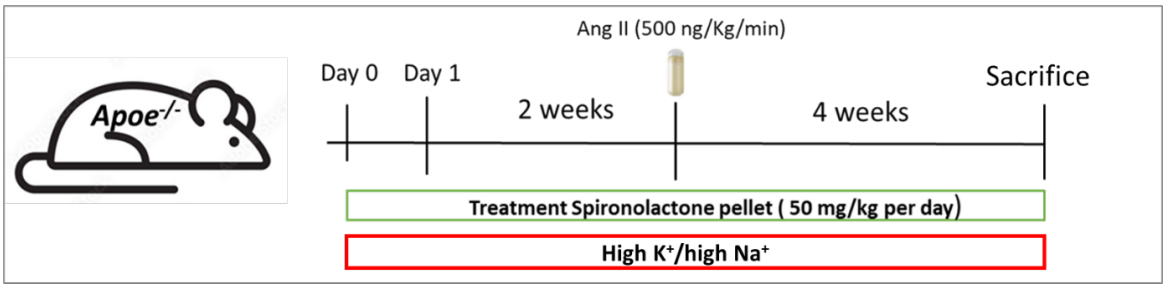

B

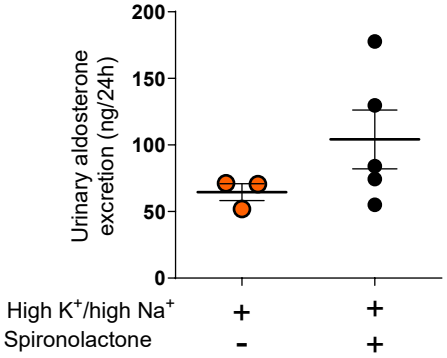

Fig. 25: (A) Animal model. (B)To validate the MR blockade, urinary aldosterone excretion of high K^+/high Na^+ fed mice treated and non-treated with spironolactone was measured before the sacrifice (64.6±6.3 vs 104.2±22.1 ng/24h). P=0.1, one-tailed t test.

3.10. Spironolactone attenuates cardiac function in Apoe $^{-/-}$ mice fed a high potassium/high sodium diet

MR blockade markedly attenuated cardiac fibrosis in high K^+/high Na^+-fed mice. Relative expression of collagen 1 and fibronectin was significantly reduced compared to non-spironolactone treated animals (0.4±0.06 vs 1±0.2 mRNA, p<0.008; 0.5±0.07 vs 1±0.2 mRNA, p<0.005). A significantly lower ANP mRNA expression was observed in spironolactone treated compared to non-treated mice (0.2±0.8 vs 1±0.3 mRNA, p<0.02). However, MR blockade did not affect the relative expression of cardiac BNP.

Spironolactone treatment resulted in a lower ventricular mass (122.6±5.3 vs 148.4±6.5 mg, p<0.006) compared to non-administered high K^+/high Na^+ mice. There was no difference in total ventricular mass. Although end-diastolic and systolic volume were similar between two groups, a slight increase of ejection fraction was observed in spironolactone treated mice. High K^+/high Na^+-fed mice receiving spironolactone had a noticeable improvement in diastolic wall thickness relative to non-spironolactone (1±0.05 vs 1.1±0.04 mg, p<0.08). Overall, MR antagonism in Ang II infused mice fed a high K^+/high Na^+ diet has beneficial effects on cardiac function.

Figure 26

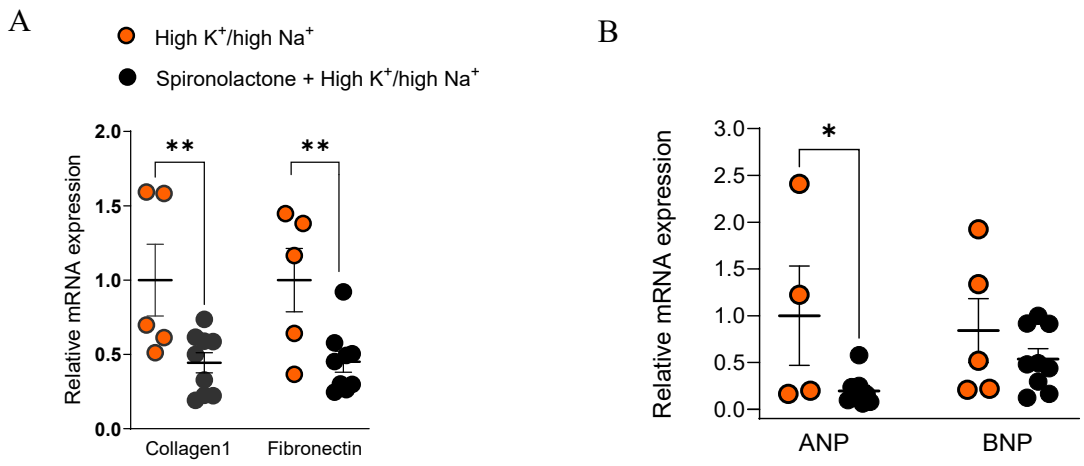

Fig.26: (A) Relative collagen and fibronectin mRNA expression of spironolactone treated (n=5) animals was significantly lower compared to non-spironolactone treated animals, respectively (0.4±0.06 vs 1±0.2 mRNA, **P<0.008; 0.5±0.07 vs 1±0.2 mRNA, **P<0.005). (B) Relative mRNA expression of spironolactone and non-treated spironolactone mice: ANP, 0.2±0.8 vs 1±0.3 mRNA, P<0.02; BNP, 0.8±0.3 vs 0.5±0.3 mRNA, P=0.2. One-tailed t test was used for comparisons.

Figure 27

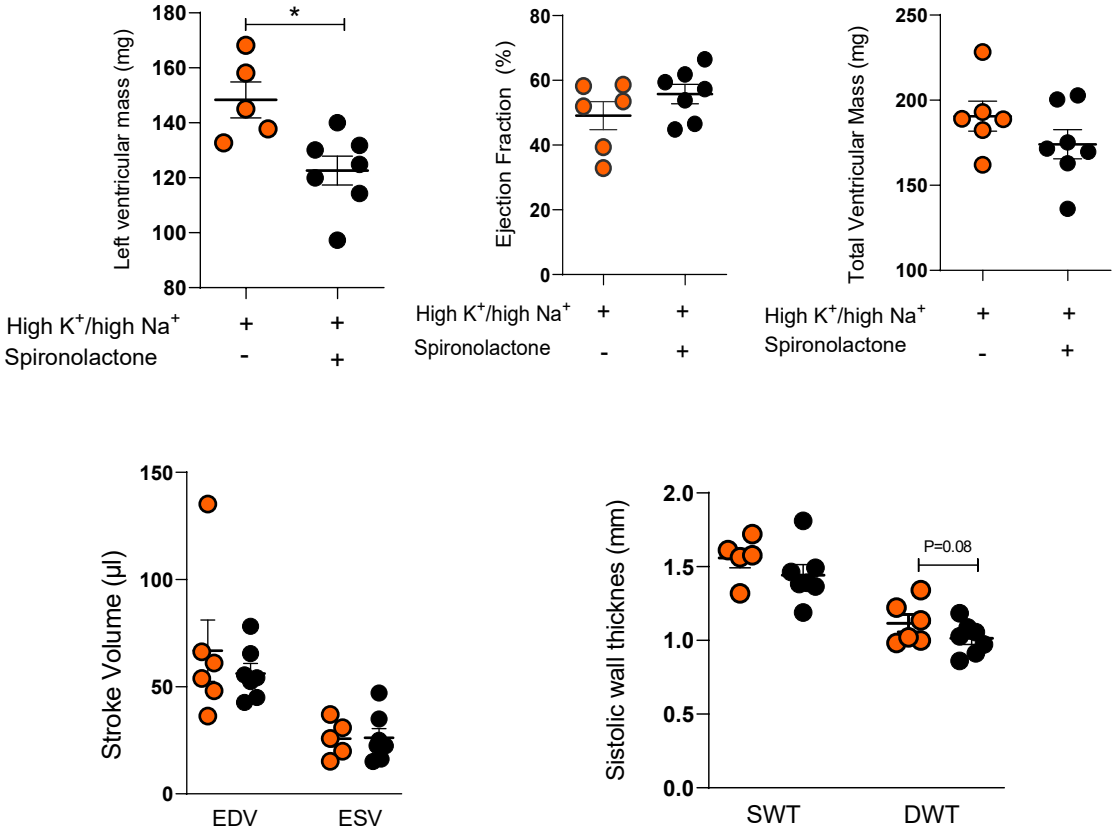

Fig.27: LVM was significantly lower in spironolactone treated mice compared to non-treated mice at the end of the experimental period (122.6±5.3 vs 148.4±6.5 mg, p<0.006). Cardiac MRI parameters, measured before sacrifice, did not differ between spironolactone (n=6) and non-spironolactone (n=7) treated mice: EF (55.8±3 vs 49.1±4.3 %, P=0.1), TVM (174±8.6 vs 190.6±8.8 mg, P=0.2), EDV (56.2±4.6 vs 66.8±14.3 ul, P=0.5), ESV (26±2 vs 25.7±3.9 ul, P=0.5), SWT (1.4±0.2 vs 1.5±0.06 mm, P=0.1) and DWT (1±0.04 vs 1.1±0.1 mm, P=0.08). One-tailed t test used.

3.11. Spironolactone reduces cardiac inflammation in Apoe $^{-/-}$ mice fed a high potassium/high sodium diet

We sought to determine whether MR antagonism decreases the inflammation in high K^+/high Na^+ fed mice. Therefore, we measured the relative expression of inflammatory cytokines in spironolactone and non-spironolactone treated mice. IL-6 secretion was significantly decreased under spironolactone intervention (0.1±0.04 vs 1±0.5 mRNA, p<0.02). MR blockade significantly lowered the expression of pro-inflammatory markers such as TNFα, IL-1β and MCP1 in the hearts of spironolactone treated mice. Whereas profibrotic marker TGFβ and iNOS were expressed similarly in both groups.

Figure 28

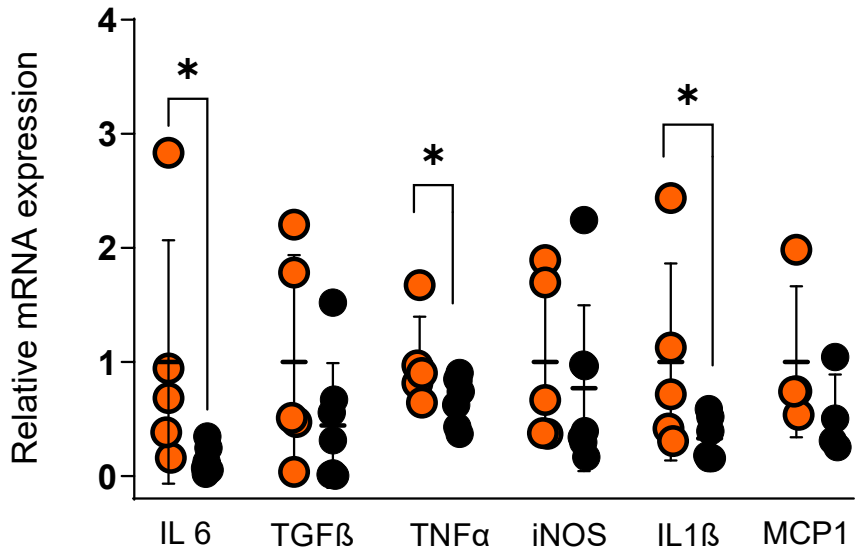

Fig.28: MR blockade with spironolactone significantly decreased the relative expression of the following inflammatory markers compared to non-treated mice: IL-6 (0.1±0.04 vs 1±0.5 mRNA, *P<0.02); TNFα (0.7±0.2 vs 1±0.04 mRNA, *P<0.04); IL-1β (0.3±0.1 vs1±0.04, *P<0.04). The relative expression of TGFβ, iNOS and MCP1 was similar between the two groups, respectively (0.4±0.2 vs 1±0.4 mRNA, P=0.2; 0.7±0.3 vs 1±0.2 mRNA, P=0.3; 0.5±0.5 vs 1±0.4 mRNA, P=0.1). One-tailed t test was used for the comparisons.

3.12. Mitochondrial function and quality assessment as a marker for senescence mediated mitochondrial ROS

As mentioned above, senescent cells contain dysfunctional mitochondria. The mitochondrial phenotype is characterized by several changes in terms of function, structure, and dynamics. First, we measured the abundance of COX4 protein, a mitochondrial content marker, and we found no significant difference among the groups (figure 29 A). Next, mitochondrial dynamics analysis displayed that high K^+/high Na^+ fed mice have more fragmented mitochondria relative to high K^+ or high Na^+ fed mice, due to the imbalance of S-OPA1/L-OPA1 protein (figure 29 B). Remarkably, treatment with spironolactone effectively lowered the S-OPA1 expression (0.95±0.1 vs 1.5±0.1 protein expression, $p<0.001$). Dysfunctional mitochondria are normally eliminated by mitophagy. The conversion from LC3BI to LC3B II reflects the cell's ability for clearance. Therefore, we quantified the ratio of LC3BI to LC3BII. High K^+/high Na^+ diet decreased significantly the mitophagy compared to high K^+ or high Na^+ fed mice. The MR blockade strikingly recuperated the clearance rate of the cardiac cells (1.2±0.2 vs 0.7±0.1 protein expression, $p<0.02$). High K^+/high Na^+ fed mice had lower ATP5A1 protein expression in comparison to high K^+ or high Na^+-fed mice. The spironolactone treatment enhanced the ATP production significantly in high K^+/high Na^+ treated hearts (1.3±0.1 vs 0.5±0.1 protein expression, $p<0.0001$).

Figure 29

A

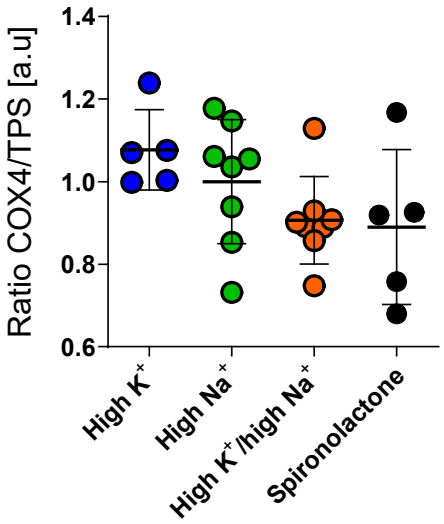

B

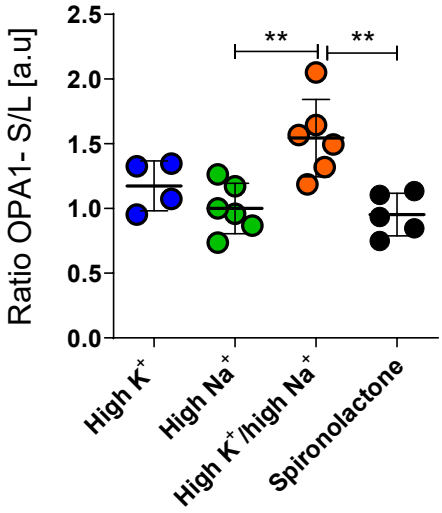

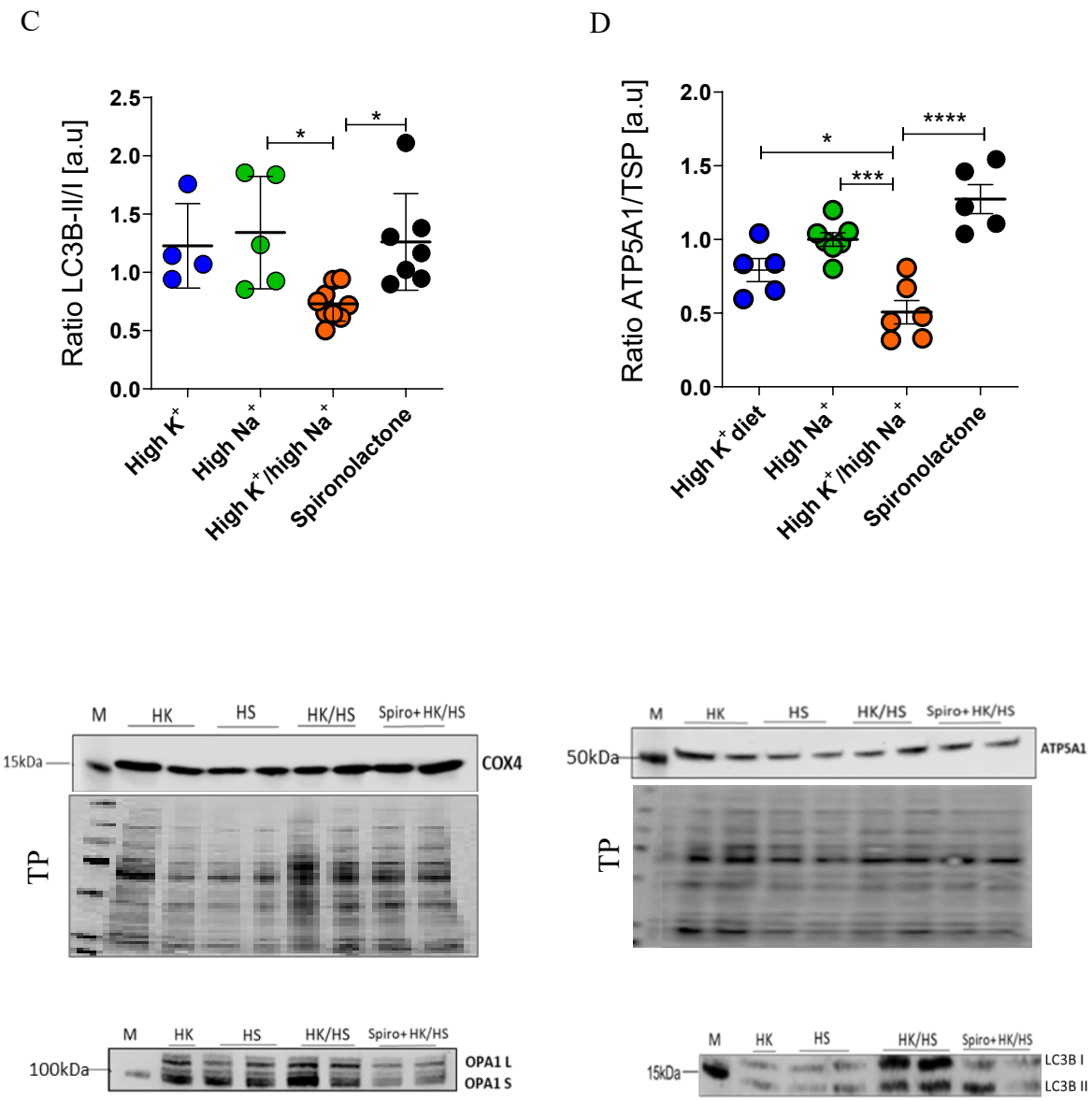

Fig.29: Mitochondrial function and quality assessment. (A) Relative expression of COX4 protein for high K^+ (n=5), high Na^+ (n=8), high K^+/high Na^+ (n=8) and spironolactone + high K^+/high Na^+ (n=5) treated animals (1±0.04 vs 1±0.05 vs 0.9±0.04 vs 0.9±0.1 relative expression, P =2.2). (B) The OPA1- S/L ratio was significantly higher in mice fed a high K^+/high Na^+ (n=6) diet compared to high K^+ (n=4) or high Na^+ (n=6) fed mice (1.5±0.1 vs 1.2±0.1 and 1.5±0.1 vs 1±0.1 relative expression, P<0.001). (C) The LC3B- II/I ratio of high K^+/high Na^+ diet (n=9) group was decreased in comparison with high K^+ (n=4) or high Na^+ (n=5) group (0.7±0.1 vs 1.2±0.2 and 0.7±0.05 vs 1.3±0.2 relative expression, P <0.01). (D) Relative expression of ATP5A1 protein was significantly lower in mice fed a high K^+/high Na^+ (n=6) compared to mice fed a high K^+ (n=5) or high Na^+ (n=7) diet (0.5±0.1 vs 0.8±0.01 and 0.5±0.1 vs 1±0.04 relative expression, P<0.04 and P<0.0002). One-way ANOVA followed by SIDAK'S multiple comparisons test. Bottom: Representative original blots. *TPS* total protein staining; *a.u* absolute units; *kDa* kilodalton; *M* marker.

4. Discussion

This preclinical study allowed us to make several novel observations: (1) chronic high K^+ diet does not provide cardiovascular protection in mice with Ang II-dependent hypertension; (2) high potassium mediated aldosterone secretion does not influence cardiovascular health; (3) the increase of K^+ and Na^+ diet concomitantly has a detrimental effect in cardiac damage of hypertensive mice; and (4) it contributes to mitochondrial dysfunction mediated senescence; lastly (5) the potassium mediated aldosterone secretion under high sodium conditions leads to cardiac damage. Our findings indicate that chronic high K^+ intake does not affect SBP and has non-beneficial effects when accompanied by high Na^+ in mice with Ang II-dependent hypertension.

4.1. The impact of high potassium diet on cardiovascular system

Dietary studies in humans and animals show that high K^+ intake reduces blood pressure (Ndanuko et al. 2021. Adv Nutr). Since the BP-lowering effect of potassium was predominantly evident in the hypertensive subjects by increasing natriuresis (Filippini et al. 2017. Int J Cardio; Dreier et al. 2020. Nephrol Dial Transplant), our initial approach was to monitor SBP in Ang II-dependent hypertension mice fed a high K^+ diet. The Ang II infusion model of experimental hypertension has been widely used in animal studies because it exhibits similarities with human hypertension, including cardiac hypertrophy or target organ damage (Lerman et al. 2019. Hypertension). Considering that the experimental period for most potassium dietary interventions in human studies has been greater than 2 weeks, the mice were maintained on a diet for six weeks in total. 2 weeks before Ang II, no significant difference was noted in SBP between 0.55 % K^+ (normal) and 5% K^+ (high)-fed mice. In the following 4 weeks, SBP was raised by about 50 mmHg in Ang II infused mice of both treatments. Surprisingly, normal and high K^+ fed mice exhibited similar SBP values.

On the other hand, increased plasma potassium also stimulates the secretion of the blood pressure-raising hormone aldosterone produced in the zona glomerulosa of the adrenal gland (Williams et al. 2005. Heart Fail Rev; Bandulik et al. 2015. Pflugers Arch). Our data showed

that potassium supplementation significantly increased plasma potassium after 6 weeks of high K^+ diet. Since plasma aldosterone levels are well represented in urinary excretion, we assessed the aldosterone excretion before and after Ang II infusion. The data showed that high K^+ diet elevated the urinary aldosterone excretion before and after Ang II significantly compared to the control diet. Our finding that high K^+ intake increased aldosterone secretion did not lead to higher Ang II-stimulated SBP rise is in agreement with the literature. Drier et al. conducted a randomized placebo-controlled double-blind crossover study in 25 healthy normotensive men, where 4 weeks of treatment with a potassium supplement (90 mmol/day) was compared with placebo. After 4 weeks, they performed an Ang II infusion experiment and the aldosterone and SBP were measured. They found that potassium-stimulated aldosterone excretion does not affect Ang II–dependent blood pressure (Dreier et al. 2021. J Am Heart Assoc).

In the aforementioned studies, increased potassium intake lowers BP in patients with hypertension (Kienker et al. 2017. Hypertension; Neal et al. 2017. Am Heart J; Bernabe-Oritz. 2020. Nat Med). The BP-lowering property of potassium has been attributed to its diuretic (thiazide-like) effect (Gritter et al. 2019. Hypertension; Aihua et al. 2023. Kidney Int Rep; Little et al. 2023. Hypertension). However, our finding demonstrates that a high K^+ diet does not alter SBP in hypertensive mice. One important aspect to be considered is the length of the studies. In short-term studies, high K^+ feeding for 4 days reduces BP in mice (Little et al. 2023. JCI Insight). Another study in humans demonstrated that an acute load of 100 mmol of K^+ led to an increase not only in aldosterone production but also in urinary excretion of potassium and sodium, highlighting the correlation of lower SBP with high sodium excretion (Buren et al. 1992. Clin Sci). In contrast, the medium/long-term studies reported that the increased K^+ intake led to high plasma aldosterone and renin, whereas there was no change in sodium/potassium excretion and BP consequently (Graham et al. 2014. J Hum Hyperten). Based on the literature, the increased plasma potassium concentration inhibits directly NCC, which increases the sodium excretion resulting in lower blood pressure. The increase in plasma potassium also stimulates the aldosterone secretion, which is known to elevate blood pressure. Our data showed that high-dietary K^+ does not affect blood pressure in hypertensive mice. One interpretation is that adaptive mechanisms are activated to balance potassium-induced sodium and water loss by activating the RAAS components. The unchanged systolic blood pressure could be due to the fact that the

potassium-mediated natriuretic effect is counteracted by a compensatory increase in aldosterone in order to compensate for the sodium loss in the long term.

In addition to the blood pressure, we measured other cardiovascular parameters and no difference was found between high and normal K^+ diet fed animals. The cardiac MRI parameters such as ejection fraction, left ventricular mass, systolic and diastolic wall thickness were similar after 6-week diet and non-significant changes in the cardiac extracellular matrix of hypertensive mice were observed among the two groups. Our data agree with a recent meta-analysis by Tang et al, which found that an increased potassium dose from 40 to 150 mmol/day did not improve pulse wave velocity and endothelial function (Tang et al. 2017. Int J Cardiol). Finally, an *ex vivo* study performed on subcutaneous resistance arteries demonstrated that higher K^+ intake did not affect endothelial function and vascular smooth muscle cell reactivity (Dreier et al. 2020. Nephrol Dial Transplant).

4.2. High potassium/high sodium induces cardiac damage in hypertensive mice

Aldosterone-induced organ damage occurs through aldosterone-MR activation in the heart, vasculature and kidney. Activation of MR in endothelial cells, fibroblasts, smooth muscle cells, podocytes and mesangial cells leads to oxidative stress, cardiac inflammation, interstitial fibrosis and renal damage. Robust scientific evidence demonstrates that aldosterone-induced hypertension and hypertensive end-organ damage is dependent on sodium (Chen et al. 2023. Hormone and Metabolic Research). This paradigm was supported by a study of the New Guinea hill tribes, who eat a very low sodium diet (2–3 mEq/day) and consequently have very high aldosterone concentrations due to RAAS activation, yet they are characterized by low blood pressure and no cardiovascular damage (Vadiya et al.2018. Endocr. Rev). The precise mechanism of how dietary sodium potentiates mineralocorticoid pathology remains unclear. However, prior studies have shown that serum and glucocorticoid-regulated kinase 1 (SGK-1) mediates mineralocorticoid/Na^+-induced damage (Sierra-Ramos et al. 2021. Am J Physiol; Beusecum et al. 2019. Hypertension). SGK-1 knockout mice when treated with excess aldosterone and high sodium show no progression of hypertension (Scaife et al. 2017. Placenta). SGK1 is an important intracellular sensor of sodium and its expression is enhanced by mineralocorticoids and glucocorticoids. In addition to regulating the expression of epithelial sodium channels, SGK1 has been found to mediate

sodium-induced T cell activation and production of IL-17A resulting in endothelial dysfunction and raised SBP (Wu t al. 2013. Nature; Norlander et al. 2017. JCI Insight).

To study the effect of mineralocorticoid excess in high sodium concentrations, several setups have been established. One of the most studied rodent models is the DOCA pellet plus high Na^+ 1 % (Basting et al. 2017. Curr Hypertens Rep) which we mimicked to uncover the effect of high aldosterone production. Therefore, we supplemented the high K^+-fed mice with high Na^+ (1% in drinking water).

Our data show that animals fed a high Na^+ diet containing normal (0.55% K^+) or high potassium (5% K^+) have higher SBP after 4 weeks of Ang II infusion compared to mice fed a high K^+ diet containing normal Na^+. This implies that the increase in BP is driven by sodium presence. This finding conflicts with the current theory that a high K^+ intake has a beneficial effect on BP in human subjects with a high Na^+ intake, i.e.>4 g/day (Aburto et al. 2013. BMJ). However, our finding replicates the study reported by (Vitzhum et al. 2014. J Physiol), where an increase in BP was observed in mice consuming a high K^+ (5%)- high Na^+ (3%) diet. One explanation could be that high Na^+ intake reduced RAAS activity in order to maximize urinary sodium excretion and in this case K^+ intake has no inhibitory effect in NCC, whereas at the same time potassium-induced aldosterone stimulates sodium retention leading to high blood pressure (Poulsen et al. 2019. J Physiol).

To examine a potential involvement of the kidney in the observed SBP, we measured sodium, potassium and aldosterone excretion. The high K^+ and the combined diet increased potassium excretion significantly compared to the high Na^+ diet. In line with the abovementioned results, high K^+ intake increased aldosterone production before and after Ang II similarly. As expected, high Na^+-fed mice had lower aldosterone amounts. High K^+ intake enhanced Ang II-induced aldosterone secretion in the presence of sodium, as evidenced by a 2-fold increase in aldosterone excretion of high K^+/high Na^+-fed mice. Additionally, the combined diet caused a greater natriuresis than the high K^+ or high Na^+ diet alone at the end of the experimental period, pointing out indirectly the natriuretic effects of potassium. However, the SBP was high in mice fed with combined diets, which is attributed to sodium presence since the blood pressure values were similar with the high Na^+ fed mice. This finding agrees with a recent study that demonstrated that after switching the aldosterone-infused rats from a low to high Na^+ diet, the blood pressure rose and remained elevated (Kurtz et al. 2023. Hypertension).

We then sought to understand whether potassium-induced aldosterone secretion plays a role in cardiac function in the context of sodium excess. The cardiac hypertrophy parameters heart/body weight and heart weight/tibia length index were significantly higher in mice maintained on high K^+/high Na^+ compared to high K^+ or high Na^+ alone. The cardiac MRI analysis revealed that mice fed with high K^+/high Na^+ had high left ventricular mass (mean = 150.9 mg) and increased diastolic wall thickness, confirming the cardiac hypertrophy finding. Our data suggest that potassium-mediated aldosterone secretion in combination with high sodium induces cardiac hypertrophy without altering SBP in hypertensive mice. From previous reports, it is controversial if aldosterone affects cardiac function through its sodium-retaining properties that alters BP or also in different ways by increasing the cardiomyocyte hypertrophy, cardiac myofibroblasts proliferation or fibroblast collagen synthesis. When rats on a low Na^+ diet were administered with aldosterone, no elevation in blood pressure was noticed. After switching to a high Na^+ diet, they became severely hypertensive and developed left ventricular hypertrophy (Brilla et al. 1992. J Lab Clin Med). Conversely, an animal study showed that aldosterone plus sodium (1%) failed to induce blood pressure modifications. Yet, it induced left ventricular hypertrophy (LVH) after 3 weeks of treatment in rats (Lopez-Andres et al. 2011. Am J Physiol). The preclinical studies corroborate these findings from human studies. Thus, it was reported by (Ohno et al. 2020. Hypertension) that aldosterone production leads to hypertrophied cardiomyocytes through its direct effect on the heart. Combination of aldosterone and high sodium increases myocardiocyte hypertrophy through reactive oxygen species-mediated mechanism, plasminogen activator inhibitor (PAI-1) and through cardiotrophin-1 mediated effect (López-Andrés et al. 2011. Am J Physiol Heart Circ Physiol; Park et al. 2004. Biochem Biophys Res Commun; Oestreicher et al.2003. Circulation). So, based on previous reports and our results, aldosterone with excessive sodium induces cardiac hypertrophy by exhibiting direct deleterious effects on the hearts of hypertensive mice.

We also observed a trend of lower ejection fraction in mice fed with high K^+ and high Na^+ diet, although not significant. This was observed particularly in mice with impaired aortic valve. These observations point to higher chance of developing heart failure with preserved ejection fraction (HFpEF) in hypertensive mice fed a high K^+/high Na^+ diet. Animal models of HFpEF are largely characterized by hypertension, left ventricular hypertrophy and diastolic dysfunction (Mishra et al. 2021. Nat Rev Cardiol). Ang II and aldosterone are among the molecular contributors to HFpEF (Nakamura et al. 2018. Nat Rev Cardiol).

Patients with HFpEF are reported to be responsive to mineralocorticoid receptor antagonism therapy (Cohen. 2020. JACC Heart Fail). Although we did not assess the diastolic function of the hypertensive mice fed a high K^+/high Na^+ diet, high left ventricular mass and diastolic wall thickness are key features of HFpEF pathophysiology.

4.3. High potassium/high sodium induces cardiac fibrosis

Inflammation and fibrosis play important roles in the pathophysiology of aldosterone-induced cardiac injury. So, we assessed cardiac fibrosis and found that high K^+/high Na^+ diet increased significantly collagen production compared to high potassium or high salt diet alone in Ang II infused mice. In response to high high K^+/high Na^+ treatment, mice myocardium displayed increased profibrotic factors, including TGF-β and tumour necrosis factor-α and upregulated expression of inflammatory cytokines such as IL-6, MCP1, IL-1β, and iNOS. Seminal studies have reported that chronic administration of aldosterone in the setting of high sodium intake causes cardiac fibrosis through perivascular and interstitial inflammation and direct alterations of extracellular matrix deposition (Lacolley et al. 2002. Circulation; Gerling et al. 2003. Am J Physiol Heart Circ Physiol; Habibi et el. 2011. Am J Physiol Heart Circ Physiol). Cell-specific overexpression and deletion of MR experiments have underlined the aldosterone-MR dependent actions. In an aldosterone-salt mouse model, overexpression of MR in cardiomyocytes and/or fibroblasts induced ventricular remodelling and fibrosis, while the deletion of MR attenuated cardiac hypertrophy and fibrosis (Bauersachs et al. 2014. Hypertens). Various animal studies have shown that aldosterone increases interstitial oxidative stress through NADPH and NFκB activation, resulting in the release of inflammatory molecules and infiltration of inflammatory cells (Buffolo et al. 2022. Hypertension). Sodium intake by itself can also promote inflammation in a manner involving TH17 cells, so a dual triggering of inflammation is necessary for aldosterone-mediated end organ damage.

4.4. High potassium/high sodium induces cellular senescence in cardiac tissues

Fibrosis has been associated with cellular senescence and persistent cardiac fibroblast senescence has shown to be deleterious (Osorio et al. 2023. Molecular Basis of Disease).

Therefore, we co-stained one sample per treatment with SA-ß-gal activity and extracellular matrix (WGA) for visualization. The representative pictures showed that fibrosis was accompanied by SA-ß-gal in several areas of myocardium of high K^+/high Na^+-fed mice. In high salt Na^+ mice, SA-ß-gal was detected in the areas of perivascular fibrosis suggesting a systemic effect dependent. Plausibly, this might reflect the sodium-increase of systolic BP in hypertensive mice. Whereas no SA ß-gal was detected in the high K^+ treated mice. The expression of IL-6, MCP1, TGFβ, TNFα are evidence of SASP, which is the main negative feedback loop of cellular senescence on tissue function and homeostasis (Gorini et al. 2019. Front. Endocrinol). Accompanied by the increase of SASP, high K^+/high Na^+ diet significantly increased the expression of cell cycle inhibitors (p16 and p21) compared to high K^+ or high Na^+ diet alone. A correlation of p21 with IL6 resulted positive, corroborating the SASP presence in mice fed with high K^+/high Na^+. These observations highlight the critical role of sodium and aldosterone excess in cardiac function during Ang II- dependent hypertension and the capability of not only inducing cardiac damage but also premature senescence.

Several studies indicate that cellular senescence is a prevalent phenotype in hypertension-associated end-organ dysfunction (Chiu et al. 2016. Twin Res Hum Genet; Westhoff et al.2008. Hypertension). McCarthy group presented a list of investigations that reported senescence in an established experimental model of hypertension or after exposure to prohypertensive stimuli (McCarthy et al. 2019. Am J Hypertens). They found a pressure-dependent association between increased cellular senescence and hypertension, with angiotensin II being the predominant pro senescence factor. Among the listed investigations, they showed that aldosterone mostly induces cellular senescence in the kidney and vasculature as an indicator of end-organ damage, but not in myocardium (Fan et al. 2011.Endocrinology; Min et al.2007. Cardiovasc. Res). To our knowledge, the role of aldosterone on premature cardiac senescence has not been directly investigated. Although a study by (Gorini et al. 2019. Front Endocrinol) revealed an association of aldosterone and cardiac deterioration in the aging setting.

One of the shared links between cardiac cellular senescence and aldosterone mediated inflammation is mitochondrial reactive oxygen species production, which drives and results from both processes and contributes to cardiac damage. Senescent cells contain dysfunctional mitochondria leading to production of excessive ROS (Passo et al. 2012. Mpl Syst Biol). Mitochondrial ROS has been shown to induce DNA damage and accelerate

telomere-induced senescence, while interventions in mitochondrial level decelerated telomere shortening (Martini et al. 2022. FEBS Journal). Regarding aldosterone stimulation of mitochondrial ROS production, an effect has been studied mostly in renal cells. However, the TAIPAI study group found that aldosterone infusion for 4 weeks supressed cardiac mitochondria in mice via MR/MAPK/p38 pathway and ROS production. The MR blockade *in vivo* prevented aldosterone-induced cardiac mitochondrial damage (Hung et al. 2022. Transl Res). Hence, we investigated the mitochondrial ROS production in the myocardium of Ang II infused mice. Given that senescence phenotype can vary across cardiac cell types, we assessed the amount of mitochondrial ROS produced by cardiomyocytes, endothelial cells and fibroblasts per each treatment. We found that mitochondrial ROS (MT/MS) in cardiac fibroblasts is significantly higher in the high K^+/high Na^+-fed mice compared to high K^+ or high Na^+-fed mice. The same trend was observed in cardiomyocyte ROS generation, where in high K^+/high Na^+- fed mice was higher than in high K^+ or high Na^+ treated mice, although not significant. On the contrary, endothelial cells produced similar amount of mitochondrial ROS among the treatments. It is in agreement with a study, which showed that aldosterone-MR activation impairs mitochondrial function in human cardiac fibroblasts via A-kinase anchor protein (AKAP-12) and this protein was downregulated in aldosterone-sodium treated rats which contributed to mitochondrial dysfunction and increased cardiac oxidative stress (Ibarrola et al. 2018. Sci Rep). Controversially, the aforementioned study from TAIPAI revealed from the *in vitro* experiment that aldosterone supresses mitochondrial ROS of cardiomyocytes. Whereas another group reported that treatment with a mitochondria-targeted antioxidant reduced mitochondrial ROS and attenuated the excess aldosterone supressed mitochondrial DNA copy numbers in endothelial cells (Hung et al. 2020. Transl Research). However, compared with our *in vivo* study, their findings are based on *in vitro* experiments.

4.5. Potassium-induced aldosterone secretion in the setting of high sodium is the main trigger of cardiac damage

Overall, we hypothesize that high potassium-mediated aldosterone binds to mineralocorticoid receptor of cardiac fibroblasts and produces mitochondrial ROS. The later

drives cardiac hypertrophy, fibrosis and premature cellular senescence on the setting of a high Na^+ diet in hypertensive mice.

To verify the hypothesis, we blocked the mineralocorticoid receptor in mice fed with high K^+/high Na^+ by using a MR antagonist. In the present study we found that spironolactone attenuated cardiac inflammation and remodelling in high K^+/high Na^+- fed mice. The left ventricular mass was reduced down to 122 mg in the spironolactone treated mice, and thus confirming the aldosterone-MR dependent effect on the heart.

To evaluate the effect of mineralocorticoid receptor antagonist on cellular senescence, we characterized the mitochondrial phenotype. Significant changes in mitochondrial dynamics, content and quality control play an important role in cell-cycle arrest and SASP (Westermann et al. 2010. Nat Rev Mol Cell Biol). Our data that S-OPA 1 protein is highly expressed in mice fed a high K^+/high Na^+ diet, indicates mitochondrial fragmentation due to dysfunctional fission. Normally, the damaged mitochondria are cleared out by mitophagy, but in the mice fed with high K^+/high Na^+ the LC3B II protein expression is significantly decreased compared to mice fed with high Na^+ or high K^+ alone. It implies that unbalanced S-OPA1 coupled with reduced mitophagy leads to dysfunctional mitochondria in myocardium of mice fed with high K^+/high Na^+ diet. Further, the cardiac mitochondria of high K^+/high Na^+ fed mice showed significantly less ATP synthase protein expression compared to high K^+ or high Na^+ alone. Interestingly, the mitochondrial mass determined by COX IV protein was similar among the treatments. These findings regarding mitochondrial phenotype in cellular senescence suggest that myocardium of high K^+/high Na^+ treated mice have more mitochondria, but they are less productive in the case of ATP synthase amount. A similar investigation, although in different setting, revealed that MR activation induces adipose tissue senescence and mitochondrial dysfunction in obese mice (Lefranc et al. 2019. Hypertens). Our data showed that treatment with mineralocorticoid receptor antagonist attenuated mitochondrial dysfunction significantly in high K^+/high Na^+ treated mice, suggesting the aldosterone-MR dependent effect on cellular senescence. Our finding agrees well with previous reports that MRA prevented aldosterone-induced cardiac mitochondrial damage *in vivo* by suppressing ROS production (Hung et al. 2020. Transl Research; Guitart-Mampel et al. 2021 Cells).

Taken together, the data from our study provide strong evidence that potassium mediated aldosterone combined with sodium causes cardiac damage and premature senescence in

hypertensive mice. Aldosterone exerts its detrimental effect via MR activation of mitochondrial ROS pathway.

It is challenging to determine if senescence is the primary driver of pathophysiology or merely a bystander. It is a focus of our interest, to investigate if the therapeutic approach of targeting senescence reverses the cardiac damage. Recent studies suggest that certain agents can prevent activation of specific mechanisms involved in cellular senescence, thus reducing the pathophysiology incidence (McCarthy et al. 2019. Am J Hypertens).

However, it should be noted that additional work is needed to characterize the role of aldosterone-MR activation on the mitochondrial dysfunction of fibroblasts. Notwithstanding to this, we cannot fully disregard the contribution of cardiomyocyte mitochondrial ROS in cellular senescence, considering that cardiomyocytes are more susceptible to mitochondrial dysfunction due to high energy requirements. Moreover, we cannot exclude the possibility that aldosterone and/or MR activation stimulates cytosolic ROS formation by increasing the NADPH oxidase activity and oxidative stress in the heart, which contributes to left ventricular remodelling following myocardial infarction (Brown et al. 2013 J Nat Rev Nephrol).

There is an extensive interest in understanding the mechanism behind the BP-lowering effect of increased potassium and the possible deleterious effects of elevated plasma aldosterone on the cardiovascular system. The data from this study provide no evidence that increased K^+ intake accompanied with elevated plasma aldosterone affect SBP and cardiovascular health in hypertensive mice. Furthermore, this study reveals that a high Na^+ diet is crucial for potassium-driven aldosterone to exert its deleterious effect on cardiovascular system. The notion of increasing potassium should be evaluated based on sodium levels because for our Western diet high in salt, may be more harmful than beneficial.

In summary, the results of the present study show that potassium stimulated aldosterone combined with excess sodium induce cardiac hypertrophy and fibrosis, as well as premature aging, in the hearts of hypertensive mice. These effects are reduced by MR blockade using spironolactone.

In conclusion, this is the first study that reports a direct link between aldosterone-MR activation, mitochondrial function, and cellular senescence in heart.

5. References

A

Aburto NJ, Hanson S, Gutierrez H, Hooper L, Elliott P, Cappuccio FP. Effect of increased potassium intake on cardiovascular risk factors and disease: systematic review and meta-analyses. 2013. BMJ. 3:346:f1378.

Alitalo K, Titze J, et al. Immune cells control skin lymphatic electrolyte homeostasis and blood pressure. 2013. J Clin Invest. 23(7):2803–2815.

Anderson AL, Harris TB, Tylavsky FA, Perry SE, Houston DK, Hue TF, Strotmeyer ES, Sahyoun NR. Dietary patterns and survival of older adults.2011: J Am Diet Assoc. 111(1):84-91.

B

Balafa O, Kalaitzidis RG. Salt sensitivity and hypertension. 2020. J Hum Hypertens. 35:184-192.

Bandulik S, Tauber P, Lalli E, Barhanin J, Warth R. Two-pore domain potassium channels in the adrenal cortex. 2015. Pflugers Arch. 467(5): 1027–1042.

Basting T, Lazartigues E. DOCA-salt hypertension: an update. 2017. Curr Hypertens Rep. 19(4):32.

Bauersachs J, Jaisser F, Toto R. Mineralocorticoid receptor activation and mineralocorticoid receptor antagonist treatment in cardiac and renal diseases. 2014.Hypertension. 65(2):257-63.

Bernabe-Oritz A. Effect of salt substitution on community-wide blood pressure and hypertension incidence. 2020. Nat Med. 26(3):374-378.

Beusecum JP, Barbaro NR, McDowell Z, Aden LA, Xiao L, Pandey AK, Itani HA, Himmel LE, Harrison DG, Kirabo A. High Salt Activates CD11c+ Antigen-Presenting Cells via SGK (Serum Glucocorticoid Kinase) 1 to Promote Renal Inflammation and Salt-Sensitive Hypertension 2019. Hypertension. 74:555–563.

Blasi E. R, Rocha R, Rudolph AE, Blomme EA, Polly ML, McMahon EG. Aldosterone/salt induces renal inflammation and fibrosis in hypertensive rats. 2003. Kidney Int. 63:1791–1800.

Brilla, CG, Matsubara LS & Weber KT. Antialdosterone treatment and the prevention of myocardial fibrosis in primary and secondary hyperaldosteronism. 1993. J. Mol. Cell. Cardiol. 25:563–575.

Brown NJ. Contribution of aldosterone ttto cardiovascular and renal inflammation and fibrosis. 2013. Nat. Rev. Nephrol. 9:459–469.

Buffolo F, Tetti M, Mulatero P, Monticone S. Aldosterone as a mediator of cardiovascular damage. 2022. Hypertension. 79:1899–1911.

C

Catena C, Verheyen ND, Url-Michitsch M, Kraigher-Krainer E, Colussi GL, Pilz S, Tomaschitz A, Pieske B, Sech LA. Association of post-saline load plasma aldosterone levels with left ventricular hypertrophy in primary hypertension. 2016. Am J Hypertens. 29(3):303-10.

Chaudhary P, Wainford RD. Association of urinary sodium and potassium excretion with systolic blood pressure in the Dietary Approaches to Stop Hypertension Sodium Trial. 2021. J Hum Hypertens. 35(7):577-587.

Chen L, Adolf C, Reincke M, Schneider H. Salt and aldosterone-reciprocal and combined effects in preclinical models and humans. 2023. Hormone and Metabolic Research.

Chiu CL, Hearn NL, Paine D, Steiner N, Lind JM. Does telomere shortening precede the onset of hypertension in spontaneously hypertensive mice? Twin Res Hum Genet 2016; 19:422–429.

Cohen JB. Clinical phenogroups in heart failure with preserved ejection fraction: detailed phenotypes, prognosis, and response to spironolactone. 2020. JACC Heart Fail. 8(3):172-184.

Cuevas CA, Su XT, Wang MX, Terker AS, Lin DH, McCormick JA, Yang CL, Ellison DH, Wang WH. Potassium Sensing by Renal Distal Tubules Requires Kir4.1. 2017. J Am Soc Nephrol. 28(6):1814-1825.

D

Dreier R, Andersen UB, Forman JL, Sheykhzade M, Egfjord M, Jeppesen JL. Effect of increased potassium intake on adrenal cortical and cardiovascular responses to angiotensin II: A randomized crossover study. 2021. J Am Heart Assoc. 10:e018716.

Dreier R, Abdolalizadeh B, Asferg CL, Hölmich L, Buus NH, Forman JL, Andersen UB, Egfjord M, Sheykhzade, Jeppesen JL. Effect of increased potassium intake on the renin-angiotensin-aldosterone system and subcutaneous resistance arteries: a randomized crossover study. 2020. Nephrol Dial Transplant. 36(7):1282-1291.

D'Sa EM, Harrison MA. Effect of pH, NaCl content, and temperature on growth and survival of Arcobacter spp. 2005. J Food Prot. 68:18–25.

E

Elijovich F, Weinberger MH, Anderson AM, Appel LJ, Bursztyn M, Cook NR, Dart RA, Newton-Cheh CH, Sacks FM, Laffer CL. Salt sensitivity and blood pressure (A scientific statement from the american heart association). 2016. Hypertension. 68: e7–e46.

Ellison DH, Welling P: Insights into salt handling and blood pressure. 2021. N Engl J Med. 385:1981-1993.

F

Fan YY, Kohno M, Hitomi H, Kitada K, Fujisawa Y, Yatabe J, Yatabe M, Felder RA, Ohsaki H, Rafiq K, Sherajee SJ, Noma T, Nishiyama A, Nakano D. Aldosterone/mineralocorticoid receptor stimulation induces cellular senescence in the kidney. Endocrinology 2011; 152:680–688.

Filippini T, Violi F, D'Amico R, Vinceti M. The effect of potassium supplementation on blood pressure in hypertensive subjects: A systematic review and meta-analysis. 2017. Int J Cardiol. 230:127-135.

Filippini T, Naska A, Kasdagli M-I, Torres D, Lopes C, Carvalho C, Moreira P, Malavolti M, Orsini N, Whelton K, Vinceti M. Potassium Intake and Blood Pressure: A Dose-Response Meta-Analysis of Randomized Controlled Trials. 2020. J Am Heart Assc. 9:e015719.

G

Gerling IC, Sun Y, Ahokas RA, Wodi LA, Bhattacharya SK, Warrington KJ, Postlethwaite AE, Weber KT. Aldosteronism: an immunostimulatory state precedes proinflammatory/fibrogenic cardiac phenotype. 2003. Am J Physiol Heart Circ Physiol. 285 (2): H813-H821.

Gorini S, Kim SK, Infante M, Mammi C, Vignera S, Fabbri A, Jaffe IZ, Caprio M. Role of aldosterone and mineralocorticoid receptor in cardiovascular aging. 2019. Front. Endocrinol. 10:3389.

Graham UM, McCance DR, Young IS, Mullan KR. A randomised controlled trial evaluating the effect of potassium supplementation on vascular function and the renin-angiotensin-aldosterone system. 2014. J Hum Hypertens. 28(5):333-9.

Greer RC, Marklund M, Anderson AM, Cobb LK, Dalcin AT, Henry M, Appel JL. Potassium-enriched salt substitutes as a means to lower blood pressure. 2020. Hypertension. 75:266-274.

Gritter M, Rotmans JI, Hoorn EJ. Role of dietary K^+ in natriuresis, blood pressure reduction, cardiovascular protection, and renoprotection. 2019. Hypertension. 73(1):15-23.

Gumz ML, Rabinowitz L, Wingo CS. An integrated view of potassium homeostasis. 2015. N Engl J Med. 373:60–72.

Guo J, Huang X, Dou L, Yan M, Shen T, Tang W, Li J. Aging and aging-related diseases: from molecular mechanisms to interventions and treatments. 2022. Signal Transduct Target Ther. 7:391.

Guyton AC, Coleman TG, Granger HJ (1972). Circulation: overall regulation. Annu Rev Physiol 34, 13–46.

H

Haberkorn SM, Jacoby C, Ding Z, Keul P, Bönner F, Polzin A, Levkau B, Schrader J, Kelm M, Flögel U. Cardiovascular magnetic resonance relaxometry predicts regional functional outcome after experimental myocardial infarction. 2017. Circ Cardiovasc Imaging. 10:e006025.

Habibi J, DeMarco VG, Ma L, Pulakat L, Rainey WE, Whaley-Connell AT, Sowers JR. Mineralocorticoid receptor blockade improves diastolic function independent of blood pressure reduction in a transgenic model of RAAS overexpression. 2011. Am J Physiol Heart Circ Physiol. 300(4):H1484-91.

Hung CH, Chang Y, Tsai CH, Liao CW, Peng SY, Lee BC, Pan CT, Wu XM, Chen ZW, Wu V, Wan CH, Young MJ, Chou CH, Lin YH. Aldosterone suppresses cardiac mitochondria. 2022. Transl Research. 239:58-70.

J

Jannone G, Rozzi M, Najimi M, Decottignies A, Sokal EM. An optimized protocol for histochemical detection of senescence-associated beta-galactosidase activity in cryopreserved liver tissue. 2020. J Histochem Cytochem. 68(4):269-278.

Jones DW, Whelton PK, Allen N, Clark III D, Gidding SS, Muntner P, Nesbitt S, Mitchell NS, Townsend R, Falkner B. Management of stage 1 hypertension in adults with a low 10-year risk for cardiovascular disease: filling a guidance gap: a scientific statement from the american heart association. 2021. Hypertension. 77:e58–e67.

Jones DW, Clark D, Morgan TO, He FJ. Potassium-enriched salt substitution as a population strategy to prevent cardiovascular disease. 2022. Hypertension. 79:2199–2201.

K

Kamel KS, Schreiber M, Halperin ML. Integration of the response to a dietary potassium load: a paleolithic perspective. 2014. Nephrol Dial Transplant. 29:982–98.

Kitada K, Nishiyama A. Potential Role of the Skin in Hypertension Risk Through Water Conservation: Salt Series. 2023. Hypertension. Volume 0: Ahead of print.

Kovesdy CP, Appel LJ, Grams ME, Gutekunst L, McCullough PA, Palmer BF, Pitt B, Sica DA, Townsend RR. Potassium homeostasis in health and disease: A scientific workshop cosponsored by the National Kidney Foundation and the American Society of Hypertension. 2017. J Am Soc Hypertens. 11(12):783-800.

Kovesdy CP, Matsushita K, Sang Y, Brunskill NJ, Carrero JJ, Chodick G, Hasegawa T, Heerspink HL, Hirayama A, Landman GWD, Levin A, Nitsch D, Wheeler DC, Coresh J, Hallan SI, Shalev V, Grams ME. Serum potassium and adverse outcomes across the range of kidney function: a CKD Prognosis Consortium meta-analysis. 2018. Eur Heart J. 39(17):1535-1542.

Krishna GG, Kapoor SC. Potassium depletion exacerbates essential hypertension. 1991. Ann Intern Med. 115(2):77-83.

Kurtz TW, Morris Jr RC, Pravenec M, Lujan HL, DiCarlo SE. Hypertension in primary aldosteronism is initiated by salt-induced increases in vascular resistance with reductions in cardiac output. 2023. Hypertension. 80:1077–1091.

Kurtz TW, Griffin KA, Bidani AK, Davisson RL, Hall JE; Subcommittee of Professional and Public Education of the American Heart Association Council on High Blood Pressure Research. Recommendations for blood pressure measurement in humans and experimental animals: part 2: blood pressure measurement in experimental animals: a statement for professionals from the Subcommittee of Professional and Public Educa-tion of the American Heart Association Council on High Blood Pres-sure Research. Arterioscler Thromb Vasc Biol. 2005; 25:e22–e33.

L

Labora JA, O'Loghlen A. Classical and nonclassical intercellular communication in senescence and ageing. 2020. Trends in Cell Biol. 30(8):628-639.

Lacolley P, Carlos L, Pujol A, Delcayre C, Benetos A, Safar M. Increased carotid wall elastic modulus and fibronectin in aldosterone-salt-treated rats effects of eplerenone. 2002. Circulation. 106:2848–2853.

Lerman LO, Kurtz TW, Touyz RM, Ellison DH, Chade AR, Crowley SD, Mattson DL, Mullins JJ, Osborn J, Eirin A, Reckelhoff JF, Iadecola C, Coffman TM and on behalf of the American Heart Association Council on Hypertension and Council on Clinical Cardiology. Animal Models of Hypertension: A scientific statement from the American heart association. 2019. Hypertension. 73:e87–e120.

Little R, Murali SK, Poulsen SB, Grimm PR, Assmus A, Cheng L, Ivy JR, Hoorn EJ, Matchkov V, Welling PA, Fenton RA. Dissociation of sodium-chloride cotransporter

expression and blood pressure during chronic high dietary potassium supplementation. 2023. JCI insight. 8(5):e156437.

Little R, Ellison DH. Modifying dietary sodium and potassium intake: an end to the salt wars?: Salt series. 2023. Hypertension. 81:00-00.

López-Andrés N, Martin-Fernandez B, Rossignol P, Zannad F, Lahera V, Fortuno MA, Cachofeiro V, Díez J. A role for cardiotrophin-1 in myocardial remodeling induced by aldosterone. 2011. Am J Physiol Heart Circ Physiol. 301(6):H2372-82

M

Maeoka Y, Su X, Wang W-H, Duan X-P, Sharma A, Li N, Staub O, McCormick JA, Ellison DH. Mineralocorticoid receptor antagonists cause natriuresis in the absence of aldosterone. 2022. Hypertension. 79:1423–1434.

Marklund M, Tullu F, Thout SR, Yu J, Brady TM, Appel LJ, Neal B, Wu JHY, Rachita Gupta. Estimated benefits and risks of using a reduced-sodium, potassium-enriched salt substitute in india: a modeling study. 2022. Hypertension. 79:2188–2198.

Martini H, Passos JF. Cellular senescence: all roads lead to mitochondria. 2022. FEBS Journal. 290(5): 1153-1393.

McDonough AA, Fenton RA. Potassium homeostasis: sensors, mediators, and targets. 2022. Pflügers Archiv – Eur J Physiol. 474:853-867.

McCarthy CG, Wenceslau CF, Webb RC, Joe B. Novel contributors and mechanisms of cellular senescence in hypertension-associated premature vascular aging. 2019. Am J Hypertens. 32(8):709-719.

McLean R. Benefits of salt substitution in care facilities for the elderly. 2023. Nat Med. 29:789–790

Messerli FH, O'Donnell M, Mente A, Yusuf S. Settling the controversy of salt substitutes and stroke: sodium reduction or potassium increase? 2022. Eur Heart J. 43(35):3365-3367.

Mente A, O'Donnell MJ, Rangarajan S, McQueen MJ, Poirier P, Wielgosz A, Morrison H, Li W, Wang X, Chen D, Devanath A, et al. Association of urinary sodium and potassium excretion with blood pressure. 2014. N Engl J Med. 371:601-611.

Min LJ, Mogi M, Iwanami J, Li JM, Sakata A, Fujita T, Tsukuda K, Iwai M, Horiuchi M. Cross-talk between aldosterone and angiotensin II in vascular smooth muscle cell senescence. 2007. Cardiovasc Res. 76:506–516.

Mishra S. Kas DA. Cellular and molecular pathobiology of heart failure with preserved ejection fraction. 2021. Nat Rev Cardiol. 18:400-423.

MorrisJr CR, Schmidlin O, Sebastian A, Tanaka M, Kurtz TW. Vasodysfunction that involves renal vasodysfunction, not abnormally increased renal retention of sodium, accounts for the initiation of salt-induced hypertension. 2016. Circulation. 133:881–893.

Mylonas A, O'Loghlen A. Cellular senescence and ageing: mechanisms and interventions. 2022. Front Aging. 29:3.

N

Nakamura M, Sadoshima J. Mechanisms of physiological and pathological cardiac hypertrophy. 2018. Nat Rev Cardiol. 15(7):387-407.

Ndanuko RN, Tapsell LC, Charlton KE, Neale EP, Batterham MJ. Dietary patterns and blood pressure in adults: a systematic review and meta-analysis of randomized controlled trials. 2016. Adv. Nutr. 7(1):76-89.

Neal B, Wu Y, Feng X, Zhang R, Zhang Y, Shi J 1, Zhang J, Tian M, Huang L, Li Z, Yu Y, Zhao Y, Zhou B, Sun J, Liu Y, Yin X, Hao Z, Yu J, Li K, Zhang X, Duan P, Wang F, Ma B, Shi W, Tanna GL, Stepien S, Shan S, Pearson S-A, Li N, Yan LY, Labarthe D, Elliott P. Effect of salt substitution on cardiovascular events and death. 2021. N Engl J Med. 385(12):1067-1077.

Neal B, Tian M, Li N, Elliott P, Yan L, Labarthe DR, Huang L, Yin X, Hao Z, Stepien S, Shi J, Feng X, Zhang J, Zhang Y, Zhang R, Wu YY. Rationale, design, and baseline characteristics of the Salt Substitute and Stroke Study (SSaSS)-A large-scale cluster randomized controlled trial. 2017. Am Heart J. 188:109-117.

Nishiyama A, Yao L, Nagai Y, et al. Possible Contributions of Reactive Oxygen Species and Mitogen-Activated Protein Kinase to Renal Injury in Aldosterone/Salt-Induced Hypertensive Rats. Hypertension 2004; 43: 841–848.

Nomura N, Shoda W, Uchida S. Clinical importance of potassium intake and molecular mechanism of potassium regulation. 2019. Clin Exp Nephrol. 23:1175–1180.

Norlander AE, Saleh MA, Pandey AK, Itani HA, Wu J, Xiao L, Kang J, Dale BL, Goleva SB, Laroumanie F, Du L, Harrison DG, Madhur MS. A salt-sensing kinase in T lymphocytes, SGK1, drives hypertension and hypertensive end-organ damage. 2017. JCI Insight. 2:e92801.

O

Oestreicher EM, Martinez-Vasquez D, Stone JR, Jonasson L, Roubsanthisuk W, Mukasa K, Adler GK. Aldosterone and not plasminogen activator inhibitor-1 is a critical mediator of early angiotensin II/NG-nitro-L-arginine methyl ester-induced myocardial injury. 2003. Circulation. 108:2517–2523

Ohno Y, Sone M, Inagaki N, Kawashima A, Takeda Y, Yoneda T, Kurihara I, Itoh H, Tsuiki M, Ichijo T, Katabami T, Wada N, Sakamoto R, Ogawa Y, Yoshimoto T, Yamada T, Kawashima J, Matsuda Y, Kobayashi H, Kamemura K, Yamamoto K, Otsuki M, Okamura S, Izawa S, Okamoto R, Tamura K, Tanabe A, Naruse M and JPAS/JRAS Study Group. Nadir aldosterone levels after confirmatory tests are correlated with left ventricular hypertrophy in primary aldosteronism. 2020. Hypertension. 75:1475–1482.

Osorio JM, Espinoza-Pérez C, Rimassa-Taré C, Machuca V, Bustos JO, Vallejos M, Vargas H, Díaz-Araya G. Senescent cardiac fibroblasts: A key role in cardiac fibrosis. 2023. BBA-Molecular Basis of Disease. 1869(4):166642.

P

Park YM, Park MY, Suh YL, Park JB. NAD(P)H oxidase inhibitor prevents blood pressure elevation and cardiovascular hypertrophy in aldosterone-infused rats. 2004. Biochem Biophys Res Commun. 313:812–817.

Parksook W, Williams GH. Aldosterone and cardiovascular diseases. 2023. Cardiovasc. Res. 119(1):28-44.

Passos JF, Nelson G, Wang C, Richter T, Simillion C, Proctor CJ, et al. Feedback between p21 and reactive oxygen production is necessary for cell senescence. 2010. Mol Syst Biol. 6: 347.

Poulsen SB, Fenton RA. K^+ and the renin-angiotensin-aldosterone system: new insights into their role in blood pressure control and hypertension treatment. 2019. J Physiol. 597(17):4451-4464.

Q

Quast C. Kober F. Becker K. Zweck E. Hoffe J. Jacoby C. Flocke V. Gyamfi-Poku I, Keyser F, Piayda K, Erkens R, Niepman S, Adam M, Baldus S, Zimmer S, Nickenig G, Grandoch M, Bönner F, Kelm M, Flögel U. Multiparametric MRI identifes subtle adaptations for demarcation of disease transition in murine aortic valve stenosis. 2022. Basic Res Cardiol. 117:29.

R

Ramos CS, Garcia S, Keskus AG, Mascolo AV, Rodríguez AE, Lima S, Hernández G, González JF, Porrini E, Konu O, Rosa DA. Increased SGK1 activity potentiates mineralocorticoid/NaCl-induced kidney injury. 2021. Am J Physiol. 4:628-643.

Reincke M, Bancos I, Mulatero P, et al. Diagnosis and treatment of primary aldosteronism. 2021. Lancet Diabetes Endocrinol; 9:876–892.

Rickard AJ, Morgan J, Tesch G, Funder JW, Fuller PJ, Young MJ. Deletion of mineralocorticoid receptors from macrophages protects against deoxycorticosterone/salt-induced cardiac fibrosis and increased blood pressure. 2009. Hypertension. 54(3):537-43.

Riphagen IJ, Gijsbers L, A van Gastel MD, Kema IP, Gansevoort RT, Navis G, Bakker SJL, Geleijnse JM. Effects of potassium supplementation on markers of osmoregulation and volume regulation: results of a fully controlled dietary intervention study. 2016. J Hypertens. 34(2):215-20.

S

Scaife PJ, Mohaupt MG. Salt, aldosterone and extrarenal Na+ - sensitive responses in pregnancy. 2017. Placenta. 56:53-58.

Sebastian A, Frassetto LA, Sellmeyer DE, MorrisJr RC. The evolution-informed optimal dietary potassium intake of human beings greatly exceeds current and recommended intakes. 2006. Semin Nephrol. 26(6):447-53.

Su XT, Yang CL, Ellison DH. Kidney is essential for blood pressure modulation by dietary potassium. 2020. Current Cardiol Reports. 22:124.

Sun J, Zhang Q, Jiang H, Guo Y-l, Zeng Y-p. Investigation on consumption of low sodium salt of Shenzhen city residents.Chin J of PHM. 2016. 32:70–71.

T

Tang X, Wu B, Luo Y, Peng L, Chen Y, Zhu J, Peng C, Li S, Liu J. Effect of potassium supplementation on vascular function: A meta-analysis of randomized controlled trials. 2017. Int J Cardiol. 228:225-232.

Temme S, Yakoub M, Bouvain P, Yang G, Schrader J, Stegbauer J, Flögel U. Beyond vessel diameters: non-invasive monitoring of flow patterns and immune cell recruitment in murine abdominal aortic disorders by multiparametric MRI. 2021. Front Cardiovasc Med. 8:750251.

Terker AS, Zhang C, McCormick JA, Lazelle RA, Zhang C, Meermeier NP, Siler DA, Park HJ, Fu Y, Cohen DM, Weinstein AM, Wang WH, Yang CL, Ellison DH. Potassium modulates electrolyte balance and blood pressure through effects on distal cell voltage and chloride. 2015. Cell Metab. 21:39-50.

Tsai CH, Pan CT, Chang Y, Peng SY, Lee PC, Liao CW, Shun CT, Li PT, Wu V, Chou CH, Tsai IJ, Hung CS, Lin YH. Aldosterone excess induced mitochondria decrease and dysfunction via mineralocorticoid receptor and oxidative stress in vitro and in vivo. 2021. Biomedicines. 9(8): 946.

V

Vaduganathan M, Mensah G, Turco JV, Fuster V, Roth GA. The global burden of cardiovascular diseases and risk: a compass for future health. 2022. J Am Coll Cardiol. 80:2372-2425.

Vaidya A, Mulatero P, Baudrand R, Adler GK. The expanding spectrum of primary aldosteronism: implications for diagnosis, pathogenesis, and treatment. 2018. Endocr Rev. 39(6):1057-1088.

Valinsky WC, Touyz RM, Shrier A. Aldosterone, SGK1, and ion channels in the kidney.2018. Clin Sci (Lond). 132:173–183.

Vitzthum H, Seniuk A, Schulte LH, Müller ML, Hetz H, Ehmke H. Functional coupling of renal K+ and Na+ handling causes high blood pressure in Na+ replete mice. 2014.J Physiol. 592(5):1139-57.

W

Wainford RD. How to reduce dietary salt intake. 2017. Hypertension. 70:1087-1088.

Wang MX, Cuevas CA, Su XT, Wu P, Gao ZX, Lin DH, McCormick JA, Yang CL, Wang WH, Ellison DH. Potassium intake modulates the thiazide-sensitive sodium-chloride cotransporter (NCC) activity via the Kir4.1 potassium channel. 2018. Kidney Internation. 93(4):893-902.

Westhoff JH, Hilgers KF, Steinbach MP, Hartner A, Klanke B, Amann K, Melk A. Hypertension induces somatic cellular senescence in rats and humans by induction of cell cycle inhibitor p16INK4a. Hypertension 2008; 52:123–129.

Wiig H, Schröder A, Neuhofer W, Jantsch J, Kopp C, Karlsen TV, Boschmann M, Goss J, Bry M, Rakova N, Dahlman A, Brenner S, Tenstad O, Nurmi H, Meervala E, Wagner H, Beck FX, Müller DN, Kerjaschki D, Luft FC, Harrison DG, Alitalo K, Titze J. Immune cells control skin lymphatic electrolyte homeostasis and blood pressure. 2017. JCI. 123(7):2803-2815.

Wilck N, Matus MG, Kearney SM, Olesen SW, Forslund K, Bartolomaeus H, Haase S, Mähler A, Balogh A, Markó L, Vvedenskaya O, Kleiner FH, Tsvetkov D, Klug L, Costea PI, Sunagawa S, Maier L, Rakova N, Schatz V, Neubert P, Frätzer C, Krannich A, Gollasch M, Grohme DA, Côrte-Real BF, Gerlach RG, Basic M, Typas A, Wu C, Titze JM, Jantsch J, Boschmann M, Dechend R, Kleinewietfeld M, Kempa S, Bork P, Linker RA, Alm RJ, Müller DN. Salt-responsive gut commensal modulates TH17 axis and disease. 2017. Nature. 551: 585–589

Wilson FH, Disse-Nicodeme S, Choate KA, Ishikawa K, Nelson-Williams C, Desitter I, Gunel M, Milford DV, Lipkin GW, Achard JM, Feely MP, Dussol B, Berland Y, Unwin RJ, Mayan H, Simon DB, Farfel Z, Jeunemaitre X, Lifton RP.Human hypertension caused by mutations in WNK kinases. 2001. Science. 293(5532):1107–1112.

Wu A, Wolley MJ, Mayr HL, Cheng L, Cowley D, Li B, Campbell KL, Terker AS, Ellison DH, Welling PA, Fenton RA, Stowasser M. Randomized trial on the effect of oral potassium chloride supplementation on the thiazide-sensitive sodium chloride cotransporter in healthy adults. 2023. Kidney Int Rev. 8:1201–1212.

Wu C, Yosef N, Thalhamer T, Zhu C, Xiao S, Kishi Y, Regev A, Kuchroo VK. Induction of pathogenic TH17 cells by inducible salt-sensing kinase SGK1. 2013. Nature. 496:513–517.

Y

Yin X, Paige E, Tian M, Li Q, Huang L, Yu J, Rodgers A, Elliott P, Wu Y, Neal B. the proportion of dietary salt replaced with potassium-enriched salt in the SSaSS: implications for scale-up. 2023. Hypertension. 80:956–965.

Yuan Y, Jin A, Neal B, Feng X, Qiao Q, Wang H, Zhang R, Li J, Duan P, Cao L, Zhang H, Hu S, Li H, Gao P, Xie G, Yuan J, Cheng L, Wang S, Zhang H, Niu W, Fang H, Zhao M, Gao R, Chen J, Elliott P, Labarthe D, Wu Y. Salt substitution and salt-supply restriction for lowering blood pressure in elderly care facilities: a cluster-randomized trial. 2023. Nature Med. 29:973–981.

Yuan Y, Chen Y, Zhang P, Huang S, Zhu C, Ding G, Liu B, Yang T, Zhang A. Mitochondrial dysfunction accounts for aldosterone-induced epithelial-to-mesenchymal transition of renal proximal tubular epithelial cells. 2012. 53:30-43.

Z

Zacchia M, Abategiovanni ML, Stratigis S, Capasso G. Potassium: From Physiology to Clinical Implications. 2016. Kidney Dis. 2(2):72-9.

6. Acknowledgment

The past four years have been an incredible journey filled with victories and failures that have allowed me to grow into a better scientist and a seasoned person. I am truly grateful for the good people who have supported me in the course of my academic journey. I am eternally indebted to my first supervisor, Prof. Johannes Stegbauer, for his strategic guidance, and invaluable mentorship throughout my PhD program. His unique expertise, constructive feedback and thought-provoking ideas have been pivotal in successful conduct of this research and growth of my academic and research skills. I am also sincerely thankful to have been surrounded by incredible scientists in Prof. Johannes Stegbauers' laboratory. Special thanks to Dr. Mina Yakoub and Dr. Masudur Rahman for their unwavering support, and suggestions from all through my project. Thanks for assisting me to quickly adopt the lab culture and for your availability particularly during ups and downs of my PhD program.

Many thanks to my second supervisor, Prof. Norbert Gerdes, for the very useful pieces of advice for the past four years especially for during the last month, which enriched my thesis. Some of the results described in this thesis would not be obtained without close collaboration with his laboratory where I was provided with amenities like FACS and Immunohistochemistry facility. I count myself very lucky, to have found a collaborator like Dr. Alexander Lang, a lab senior in the group of Prof. Norbert Gerdes, who has taught me about senescence as much as about working efficiently. Thank you for your critical perusal of my thesis, and for stimulating conversations on science and for sharing your problem-solving perspective with me.

I would like to express my sincere gratitude to the head of IRTG 1902, Prof. Axel Gödecke, for funding my PhD program, enabling me to attend international conferences and for granting me a 6-month fellowship at University of Virginia, USA. I am much grateful to Brant Isakson PhD for hosting me in his laboratory in Cardiovascular Research center of the University of Virginia. His scholarly suggestions, encouragement and kind treatment have been a source of inspiration for me. I owe a special thanks and appreciation to the coordinator of IRTG 1902, Dr. Sandra Berger, for all her support from the beginning of my arrival in Düsseldorf, until very end. Sandra, thank you for the generous care and giving the homely feeling.

I was fortunate to encounter many academic colleagues and make lasting friendships - a big thank to Hend, Fatima, Imane, Era, Ava, Kaoutar, Randa, Barbs, Yasmina for all the ways

you have enriched my PhD journey. A heartfelt thank you to my bestie, Amanda, for providing the laughter, support and encouragement I needed to keep going and reminded me that I was never alone in this endeavor. I am profoundly grateful to have you in my life.

Finally, I would like to acknowledge how grateful I am for having a group of people in my life who have always believed in me more than I could believe in myself and cherished all my successes. A big thank to my wonderful husband Rafi, who has unconditionally supported me in the entirety of my academic journey, who has accompanied me to the lab at midnights, who has masterly cooked for me to eat after long hours of experiments, and who always understood me when I had to re-prioritize unilaterally our plans in the interest of my experiments. More importantly, he has always been a source of inspiration and motivation backing me to accomplish my PhD despite challenges. I am incredibly blessed to have you in my life as my great man and rock. I am the luckiest sister to have two lovely siblings who have made my journey more joyful: you have been my sweetest escape and detachment when work was overwhelming. Last but not least, I would like to thank my parents, to whom I dedicate the thesis. Your unconditional sacrifice, love and support have been decisive for me to achieve this challenging yet well-worth PhD award. I know it is impossible to compensate a glimpse of your dedications, sacrifices and unconditional love, but I hope I have made you proud.